Experimental Determination of Phase-Equilibria and Thermo-Physical Properties at Temperatures up to 3000°C by Aerodynamic-Acoustic Levitation

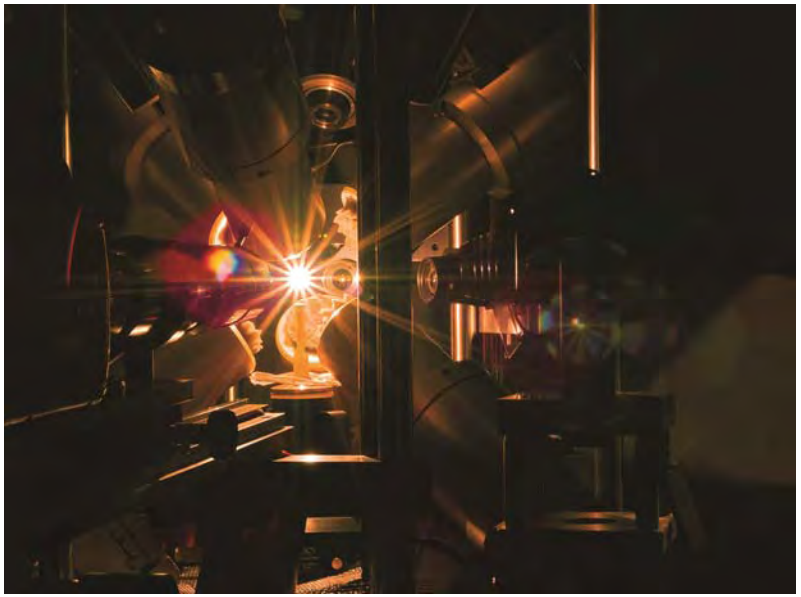

Arno Kaiser, Robert Prieler, Rainer Telle
RWTH Aachen, Institute of Mineral Engineering, Germany
Paul Nordine
Physical Property Measurements, Inc., Evanston, USA

Aero-Acoustic Levitation - Method

Acoustic Levitation + Aerodynamic Levitation

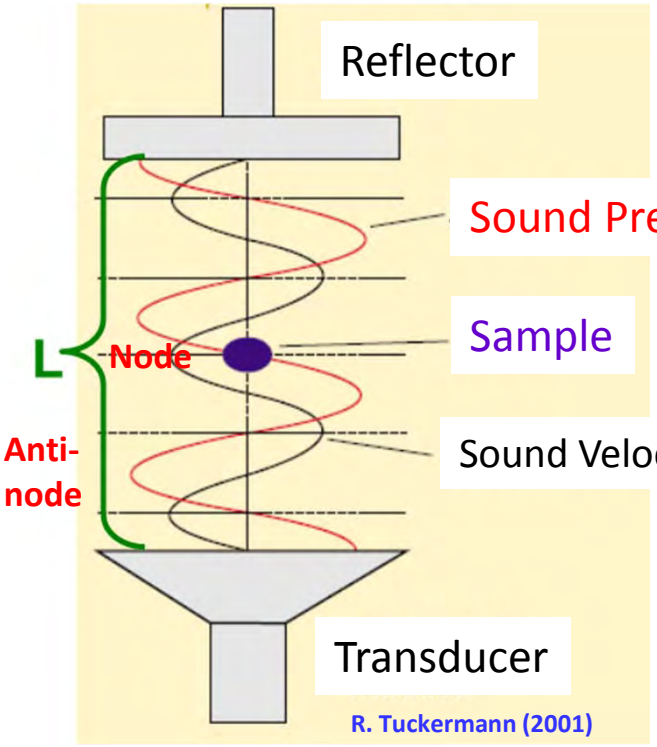

Resonance $L = n \cdot \frac{1}{2} \lambda$

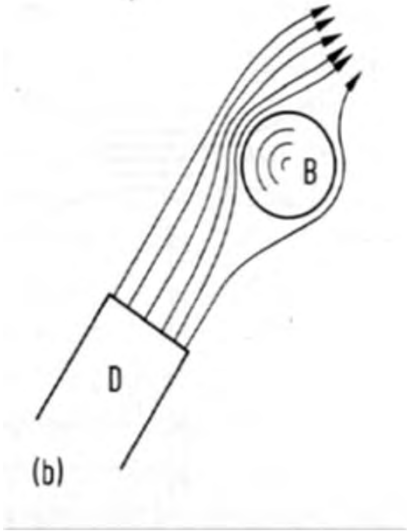

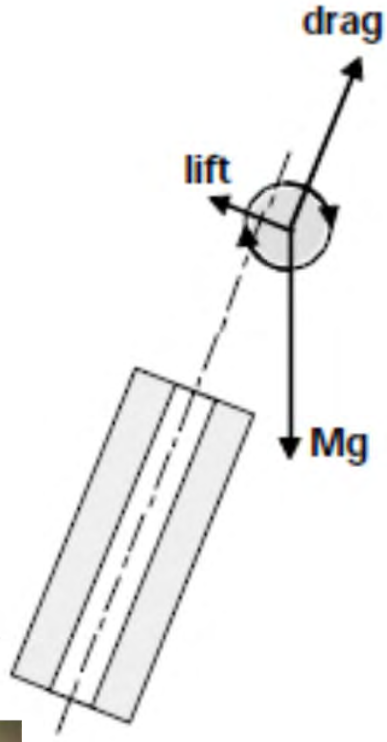

Aero-Acoustic Levitation - Method

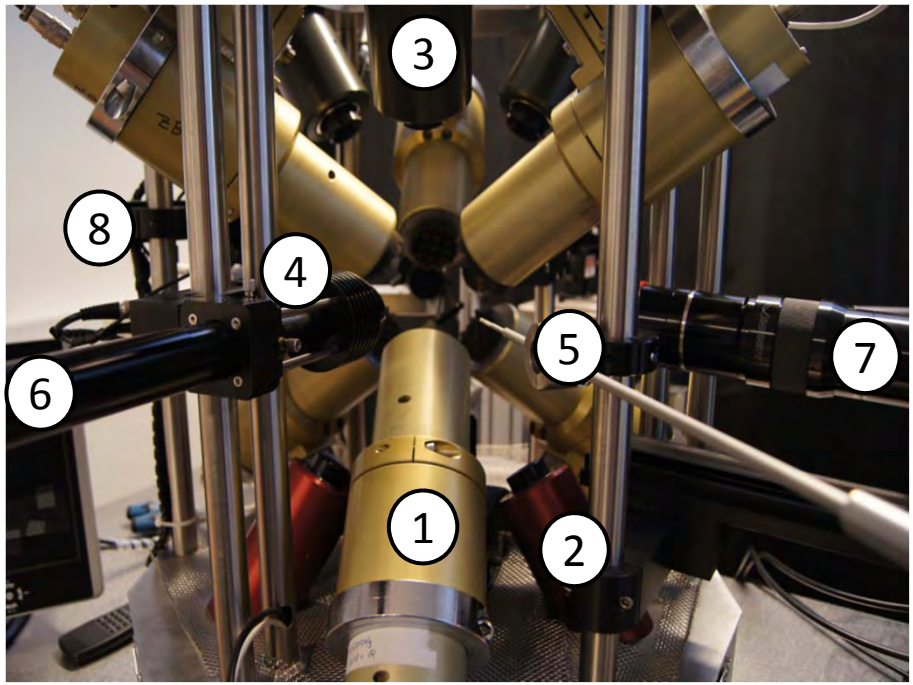

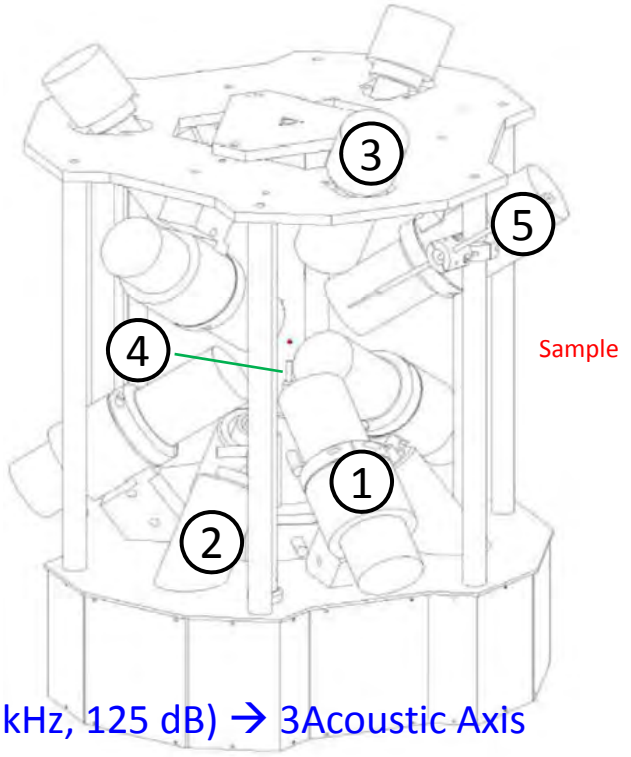

1: 6 Electroacoustic Transducers on 3 Orthogonal Axis (piecoelcetric, 22 kHz, 125 dB) → 3Acoustic Axis
2: 3 Position Sensor Lasers (808 nm diode lasers)
3: 3 Position Sensitive Detectors → Combination of spectral, spatial and temporal filtering
→ Transmission of positions status to the acoustic control system at a rate of 250/sec.
4: Gas Jet Assembly (Heated Mullite Gas FlowTube, 5l/min., 500-600°C → laminar gas flow; N_2, Ar, Air, O_2, …
5: Specimen Injector (Vacuum Chuck)
6: 2 240 W cw-CO_2-Laser (two-sided sample heating)
7: High Speed Video Camera (14-bit image depth, 1000 frames/sec. at a full resolution of 1632 x 1200 pixels
+ long-distance microscope lens (full-screen images of levitated 3 mm diameter samples)
8: Exactus pyrometer, 700°C to 3500°C, Spot Size: 0.67 mm, λ = 650 nm at measuring distance of 150 mm,
Measuring speed up to 1000 Hz, Accuracy T < 2600°C ± 1.5°C or ± 0.15% of measured temperature

- 3 orthogonal acoustic axis (3 Standing Waves)
- Control of the **position of nodes and anti-nodes** in the standing waves depends on intra-axis phase differences (automatic controlled by the acoustic control system)

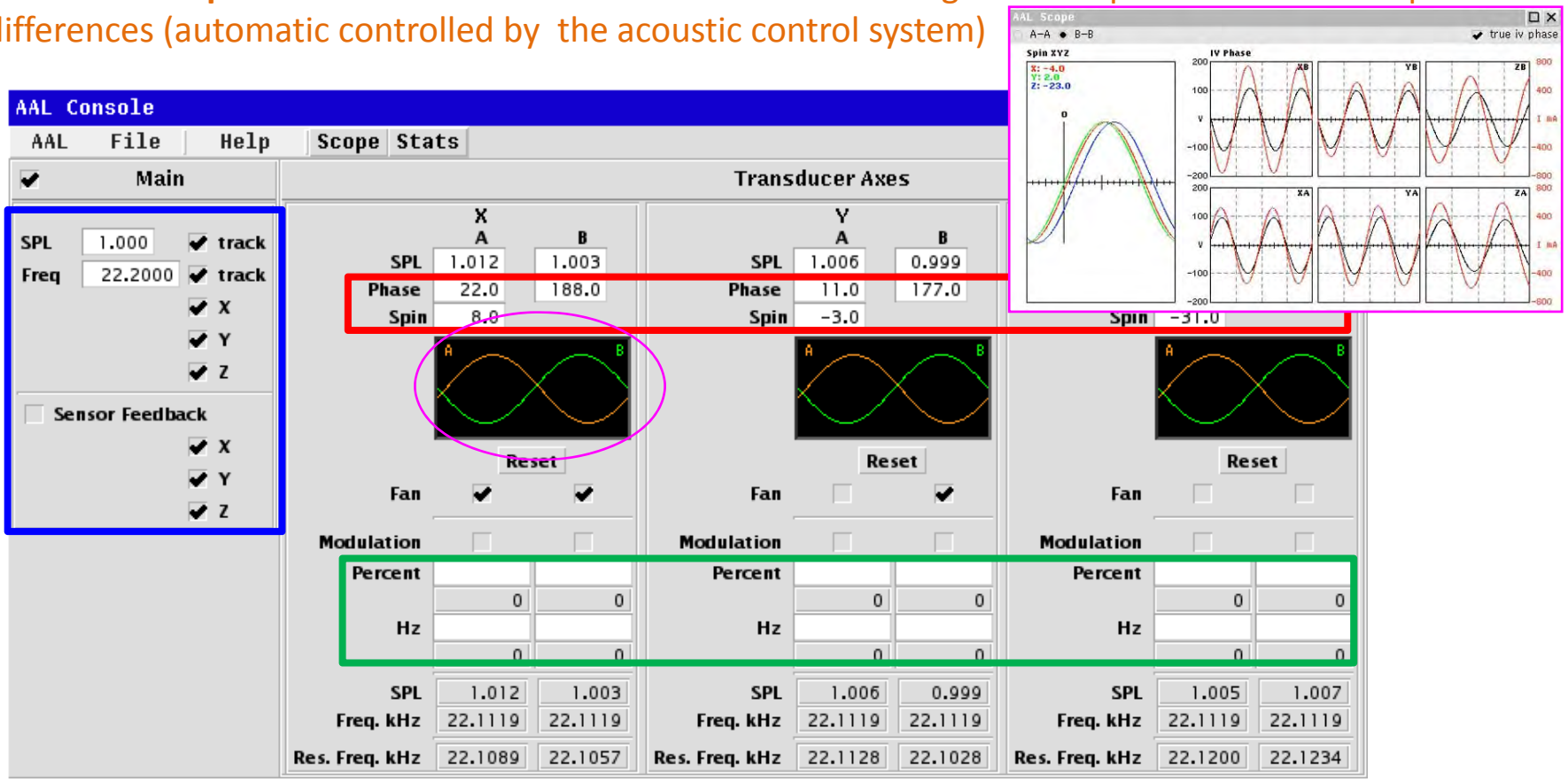

- Control of **sample rotation** through control of phase differences between the 3 orthogonal acoustic axes (Torques / Moments on a levitated sample result from inter-axis phase differences)

- Control of **sound pressure and frequency**

- Control of acoustic forces to induce **dynamic oscillation** on liquid drop by amplitude modulation of the acoustic forces → SurfaceTension, Viscosity

Advantages of Aero-Acoustic Levitation

- ***Crucible-Free, Contactless Method***

  → No contamination by crucible materials
  → Prevention of heterogeneous nucleation (Undercooled & Non-Equilibrium Melts)
  → Synthesis of high purity materials
  → Synthesis of glasses of compositions with none or little tendency to glass formation
  → …

- ***Direct Access to the Sample Surface***

  → Direct laser beam heating of the sample
  → Very high temperatures (T > 3000°C)
  → Fast heating and cooling of the Sample
  → Fast surface and bulk transport → Equilibrium
  → Direct and contactless measurements at sample surface (+ Oberservation)
  → Pure, unalterated melt surface (volatile impurities evaporate)
  → Examination of surface reactions in an reactive environment (Reactive Gases)
  → Acoustic manipulation of the levitated melt along single or all three acoustic axis → Surface Tension, Viscosity

Advantages of Aero-Acoustic Levitation

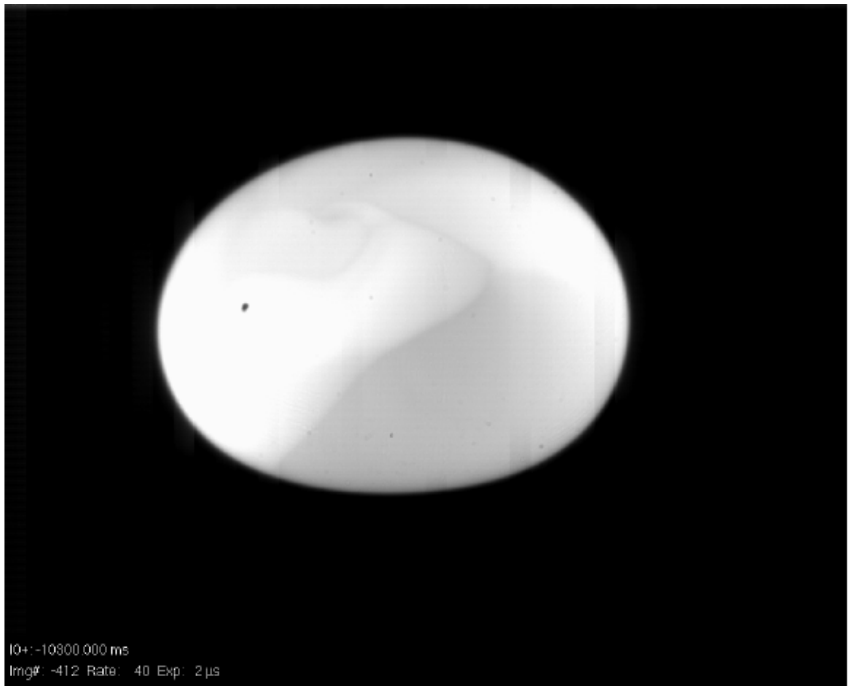

HfO_2, T_a = 2910°C

Al_2O_3, T_a = 3200°C

Density ≈ 9.6 g/cm^3

Density ≈ 3.9 g/cm^3

Applications of Aero-Acoustic Leviation

- ***Determination of thermophysical and thermochemical properties***

  → Density, Thermal Expansion, Viscosity, Surface Tension, Electrical Conductivity, …
  → Melting Points, Liquidus Temperatures
  → *Structural Properties of Levitated Melts (e. g. HT-Raman Spectroscopy)*
  → *Thermo-Optical Properties of Levitated Melts (e.g Emmissivty)*
  → …

- ***Materials Science***

  → Materials with Novel and Unusual Microstructures (Eutectic Mictostructures)
  → Materials Development
  → Nucleation and Growth, Dendritic Growth , …. → Crystal Growth
  → Phase Transitions in the Liquid and Solid state
  → Glass Formation → New Glass Materials
  → Metastable Equilibria, Phase Selection
  → Phase Separation in Melts
  → …

Sample Preparation

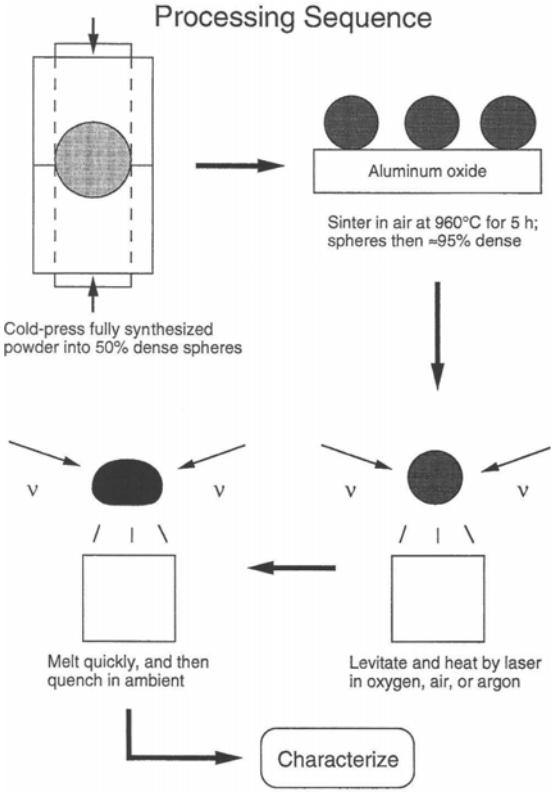

J. K. R. Weber et al. (1994)

Calibrated spheres are made by melting a weighted amount of material

$$m = \rho\pi\frac{D^3}{6}$$

Diameter, Mass, Density

D_{max} = ½ Distance between the Nodes
= ¼ λ = f(Levitation Gas)

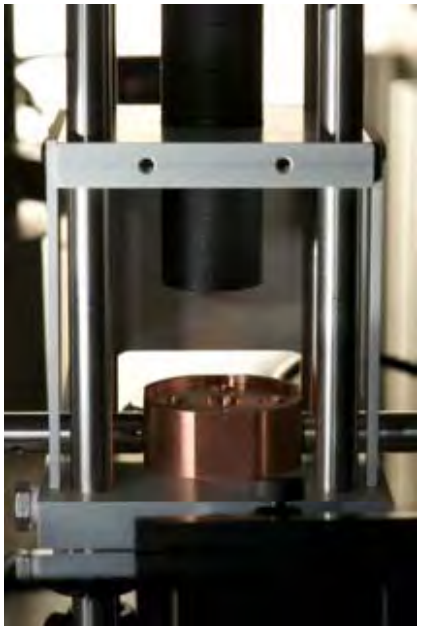

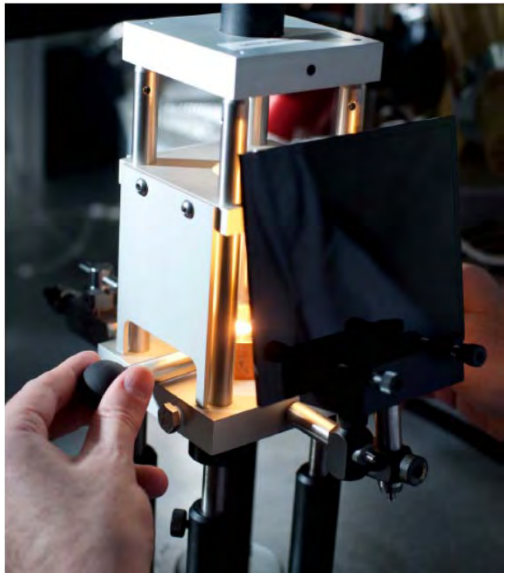

ZrO_2 $Gd_2Zr_2O_7$ $ZrSiO_4$

Al_2O_3 - Cooling Sequenze

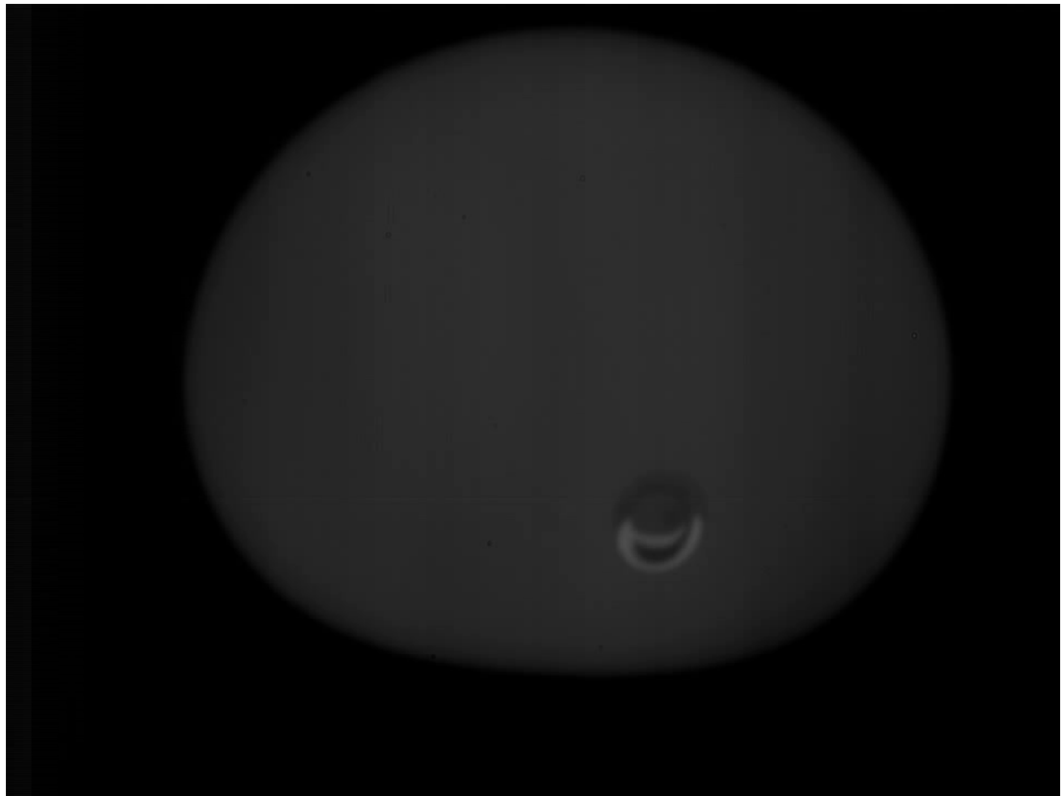

Al_2O_3 - Cooling Sequenze

700 µs

Al_2O_3 – Cooling Curve

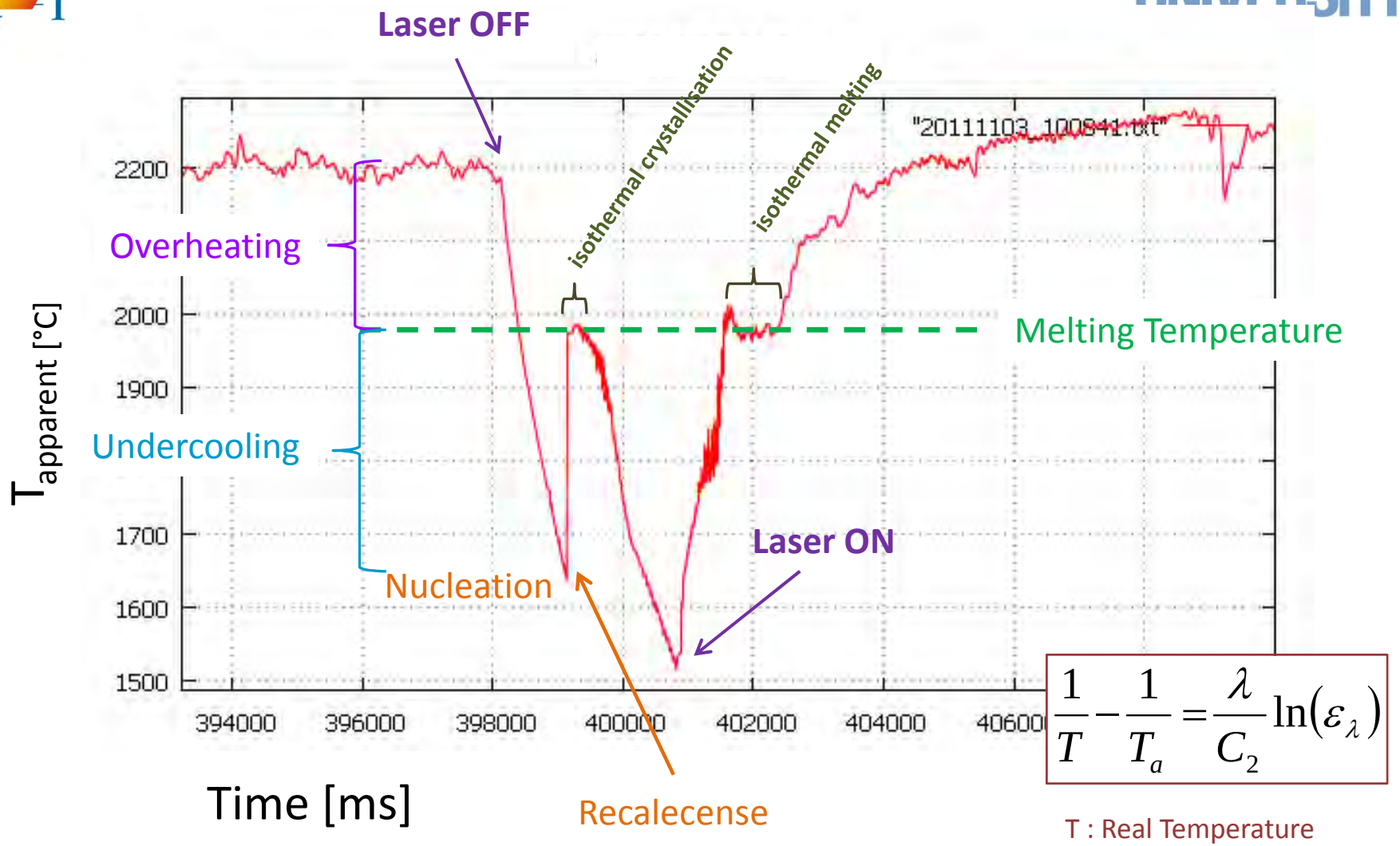

$$\frac{1}{T}-\frac{1}{T_a}=\frac{\lambda}{C_2}\ln(\varepsilon_\lambda)$$

T : Real Temperature
T_a : Measured Temperature
$C_2 = 1.4388 \cdot 10^{-2}$ m·K
λ : wavelength pyrometer
ε_λ : spectral emmisivity

Al_2O_3 Cooling Curves : High Reproducibility

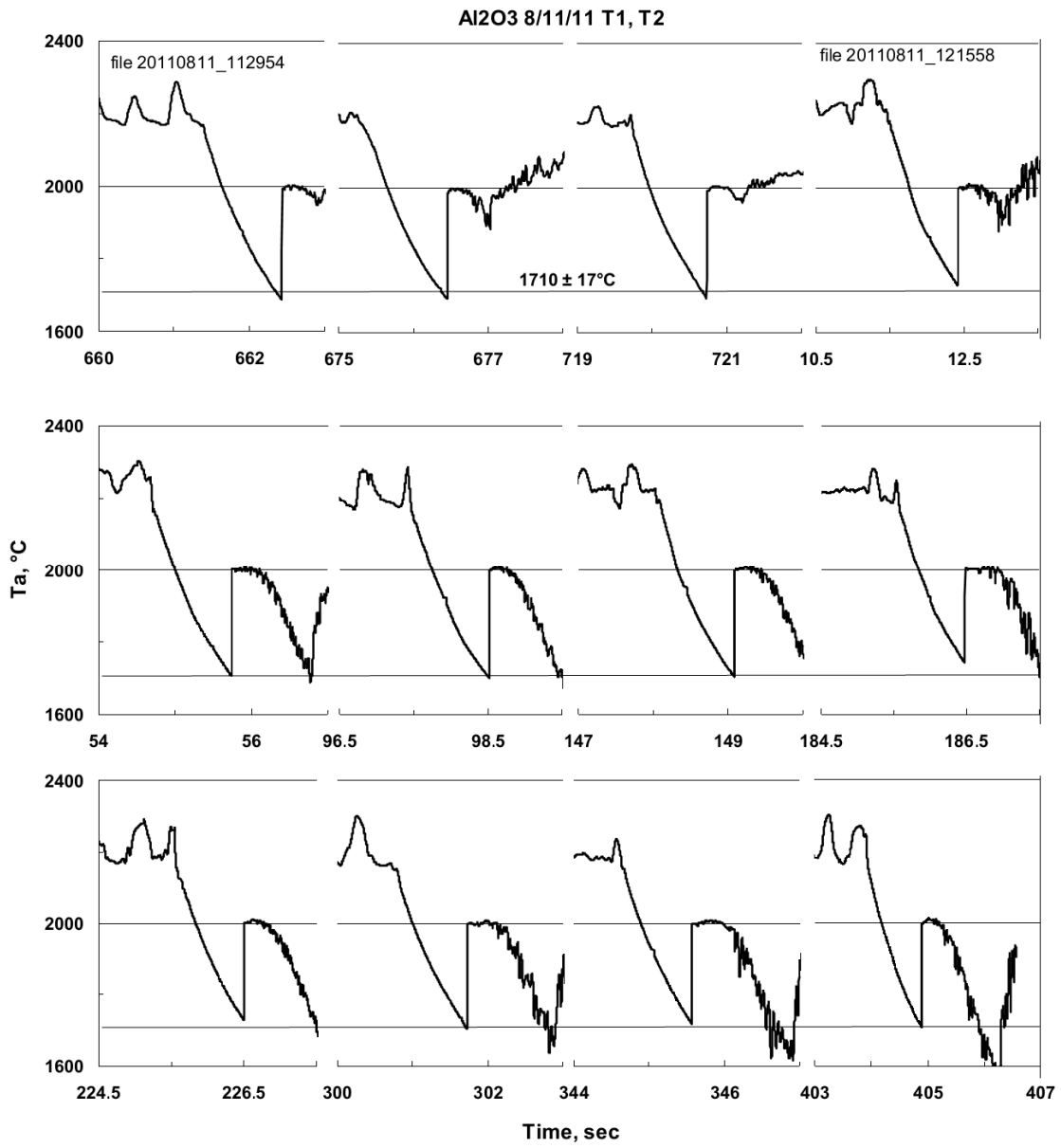

Levitation Gas : Air

Recalescense
at ~1710°C

Al_2O_3 Cooling Curve : High Reproducibility

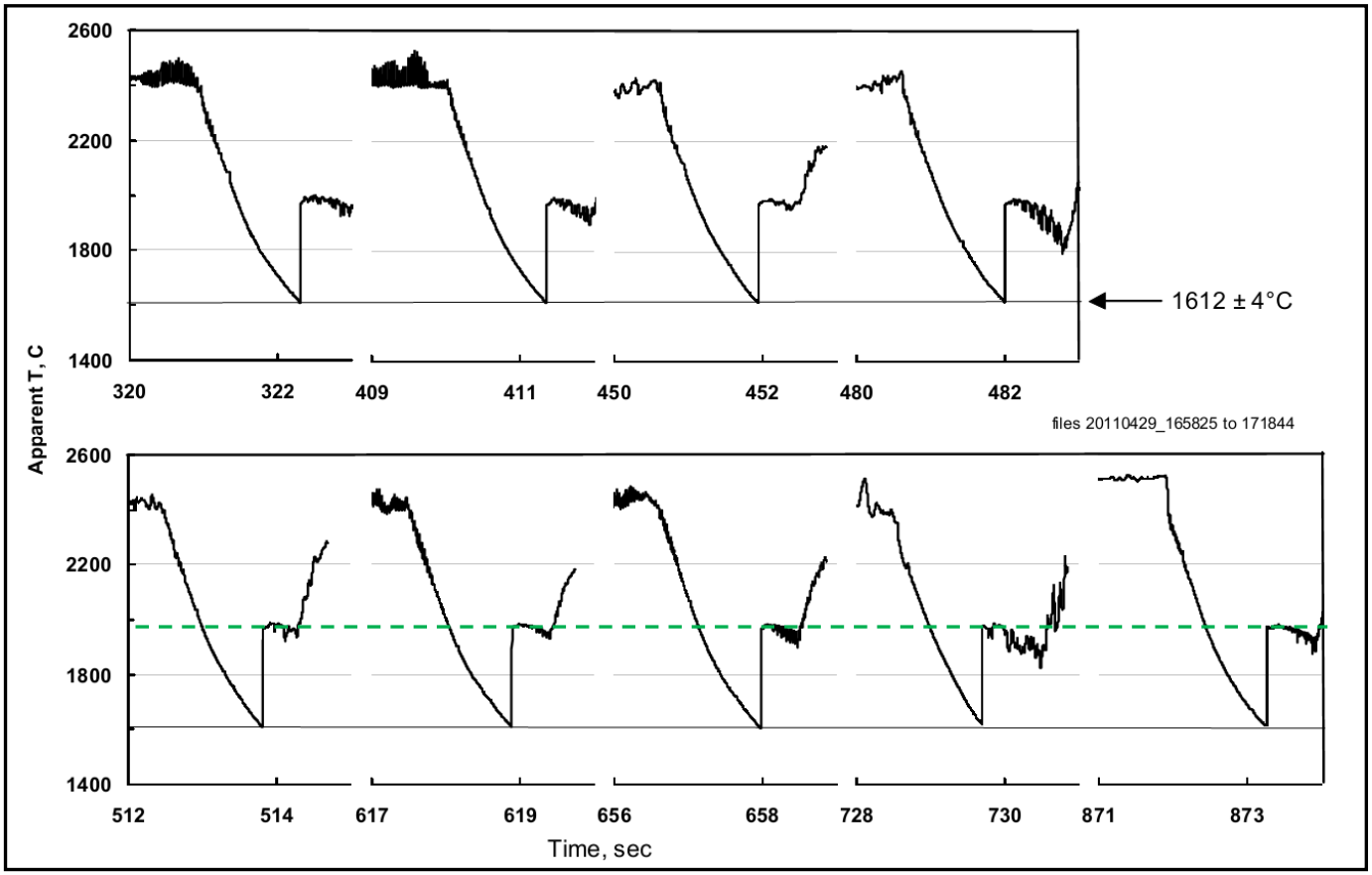

Levitation Gas : N_2

Recalescense
at ~1612°C

Al_2O_3 Microstructures

Levitation Gas : N_2

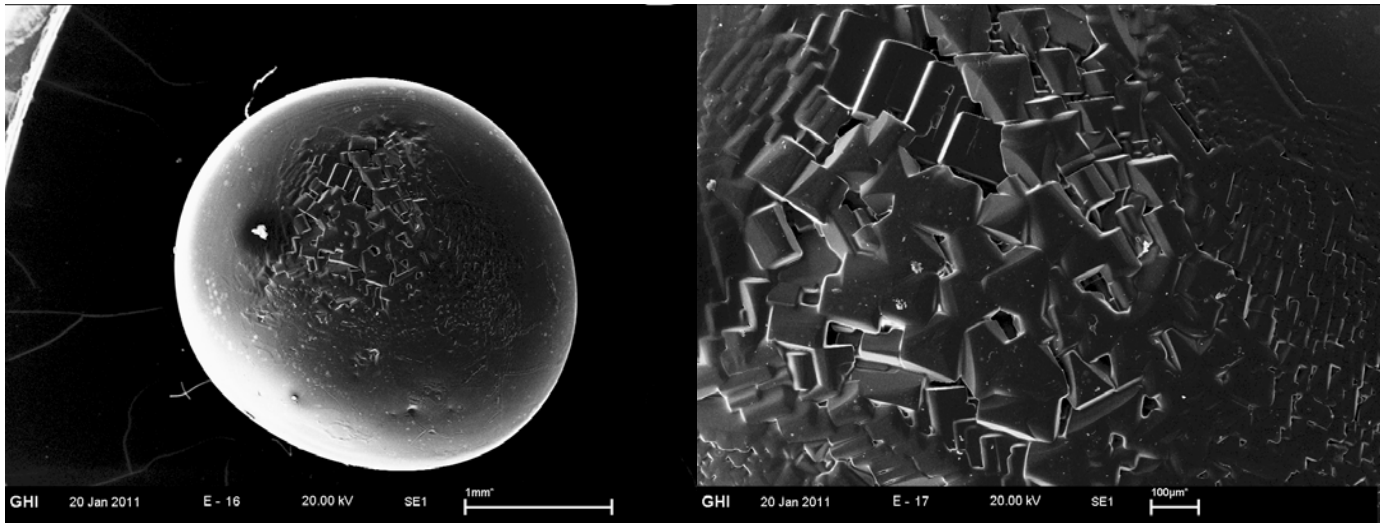

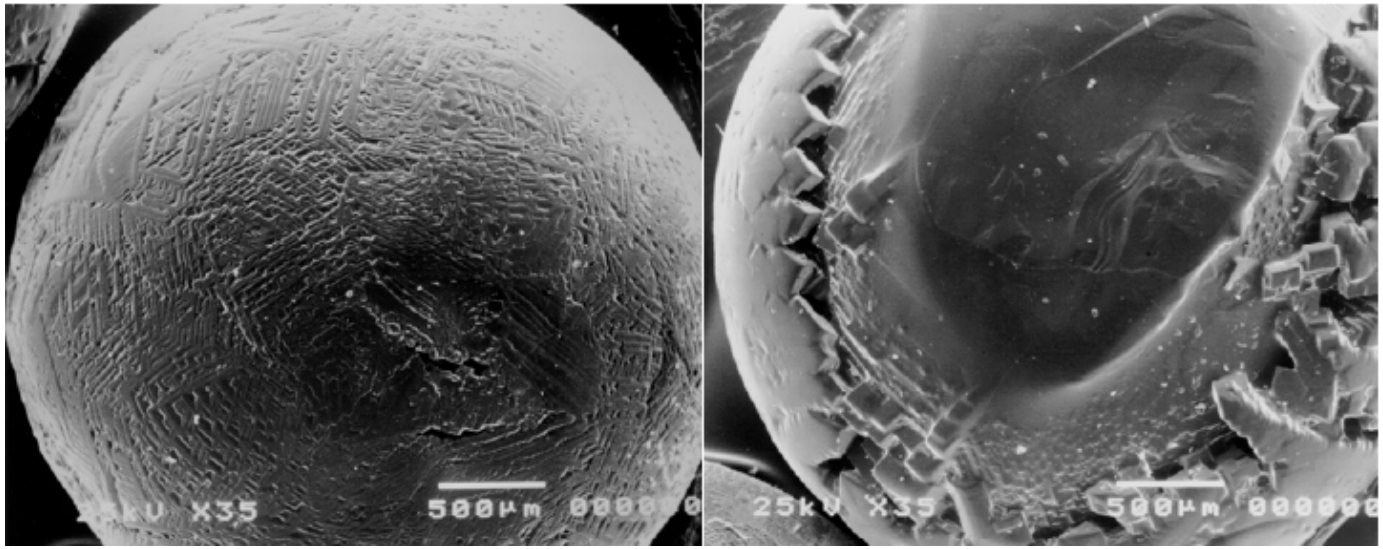

Levitation Gas : O_2

Leviation Gas : Ar

Stinger Experiments

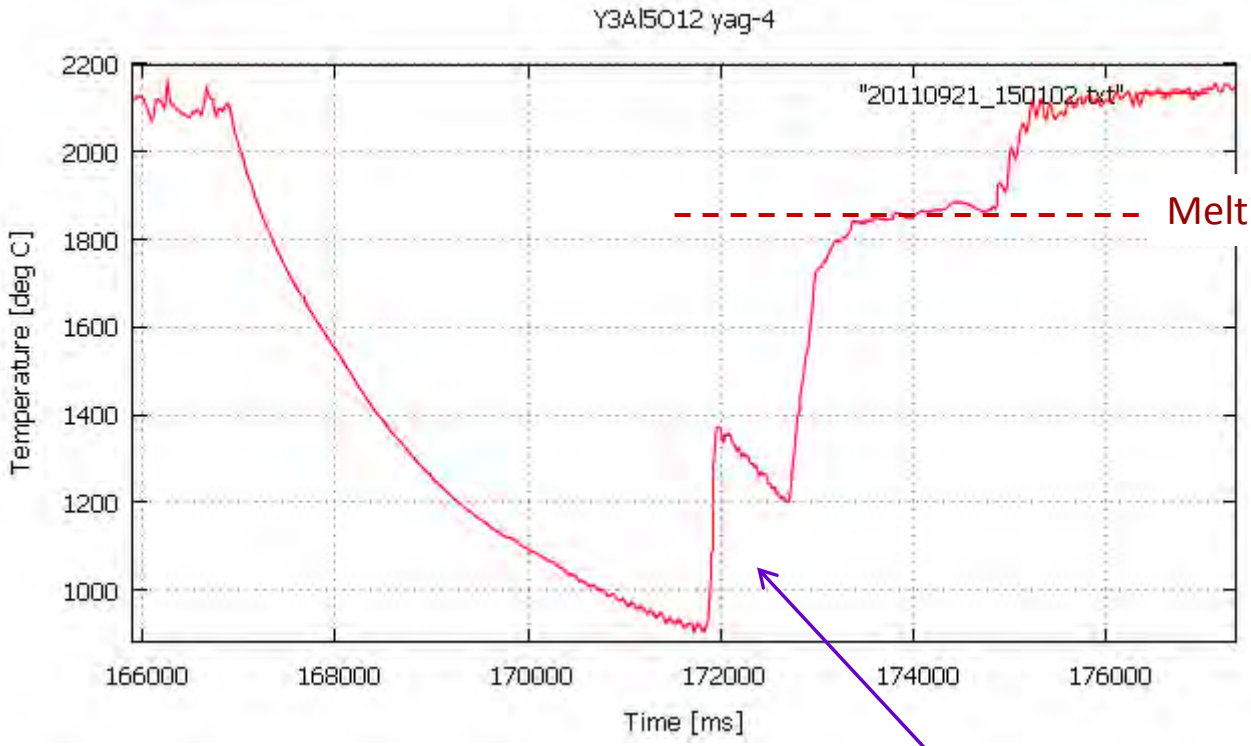

Melting Temperature

Recalescense : Sample not heated to Melting Temperature → Stinger-Experiment

Melting Temperatures – Stinger Technique

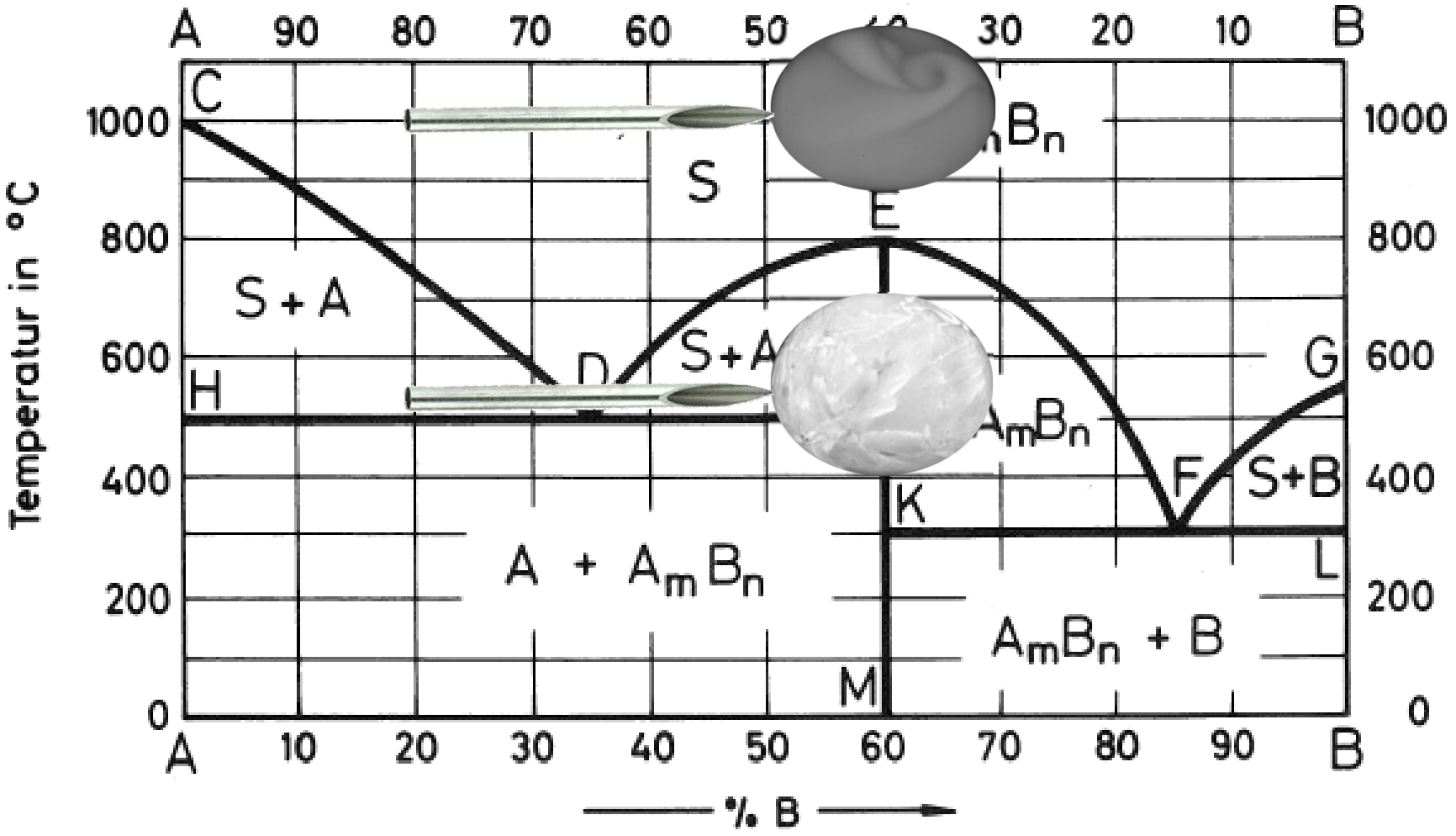

Ir- and Sapphire-Stinger

Melting Temperatures – Stinger Technique

Touching Surface of Undercooled Al_2O_3 with Ir-Stinger → Rapid Solidification

Nucleation triggered with a Ir-Stinger

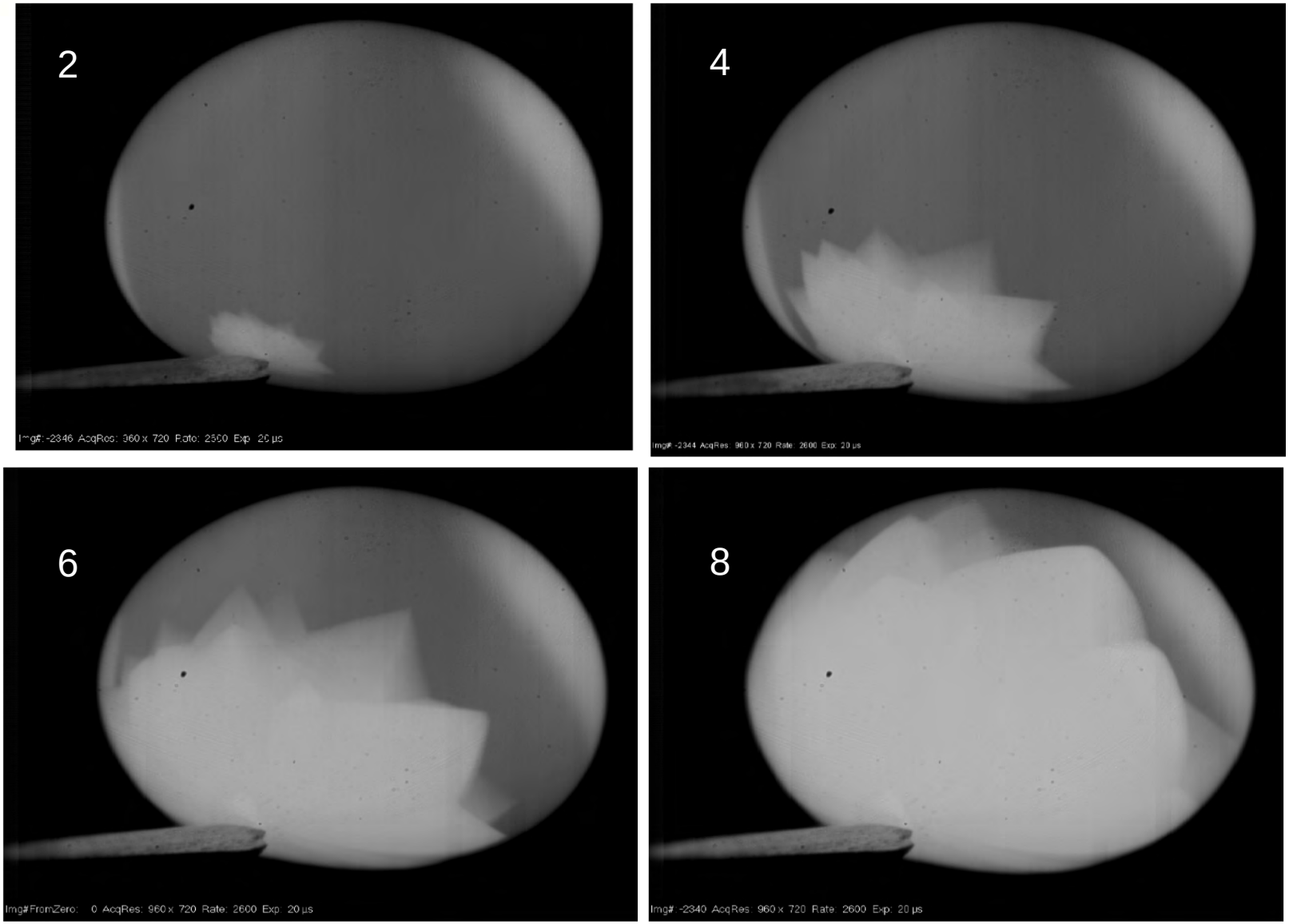

40 µs from picture to picture

Melting Temperatures – Stinger Technique

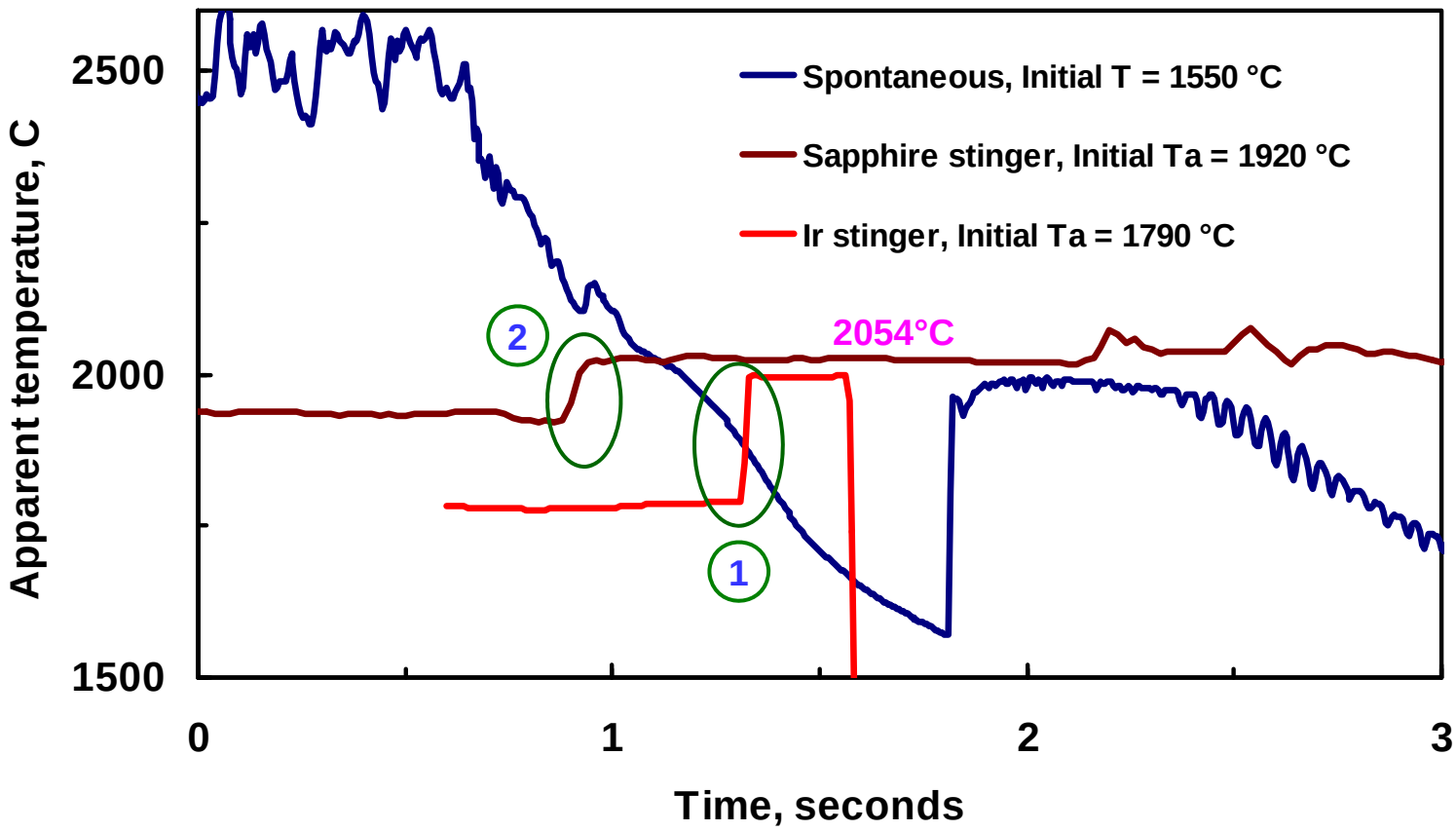

Video (1) : Crystallization of undercooled Al_2O_3, triggered with Iridium-Needle

Video-Frequency = 2600 Hz , Time of Crystallization = 4.6 ms (12 Pictures)

Crystallization-Velocity ≈ 70 cm/Second

Crystallization Rate of Undercooled Al_2O_3

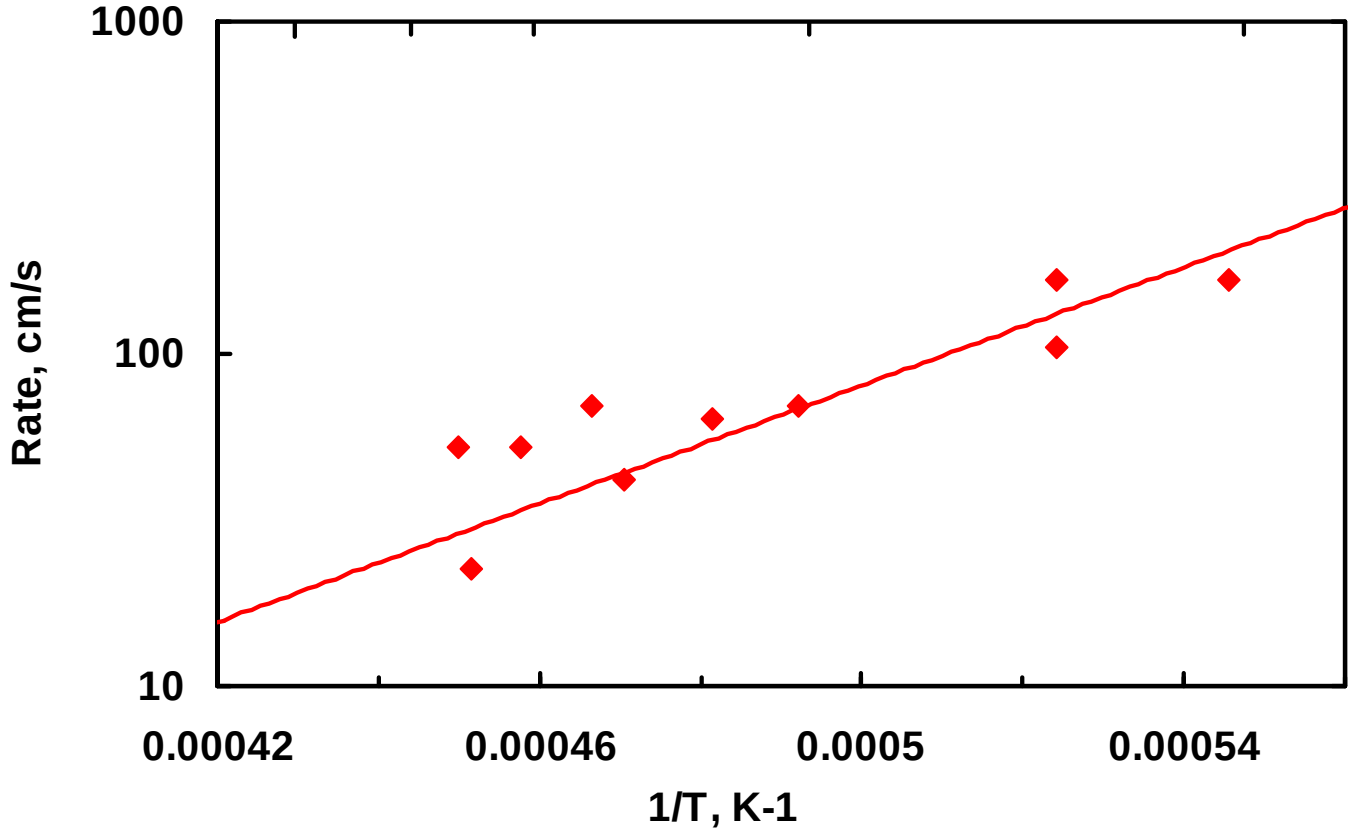

Crystallization rate of undercooled, liquid Al_2O_3
as a function of temperature

$Y_3Al_5O_{12}$ YAG

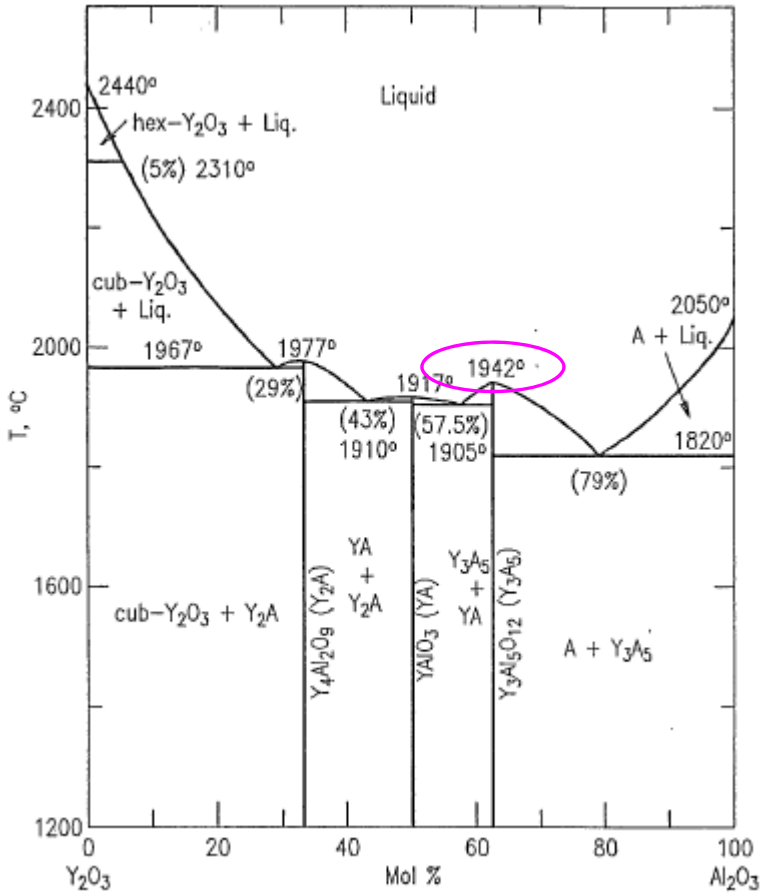

Phase Diagram Y_2O_3-Al_2O_3

Roth, R. S.,Phase EquilibriaDiagrams: PhaseDiagrams for Ceramics,Vol XI. The American Ceramic Society, Westville, OH, 1995, p. 107.

$Y_3Al_5O_{12}$ YAG

Video: slow crystallization of $Y_3Al_5O_{12}$ at T ≈ 1200°C
Δt = 0.48 seconds, frame rate 2600 Hz, sample rotation ≈ 5.3 Hz

$Y_3Al_5O_{12}$ YAG

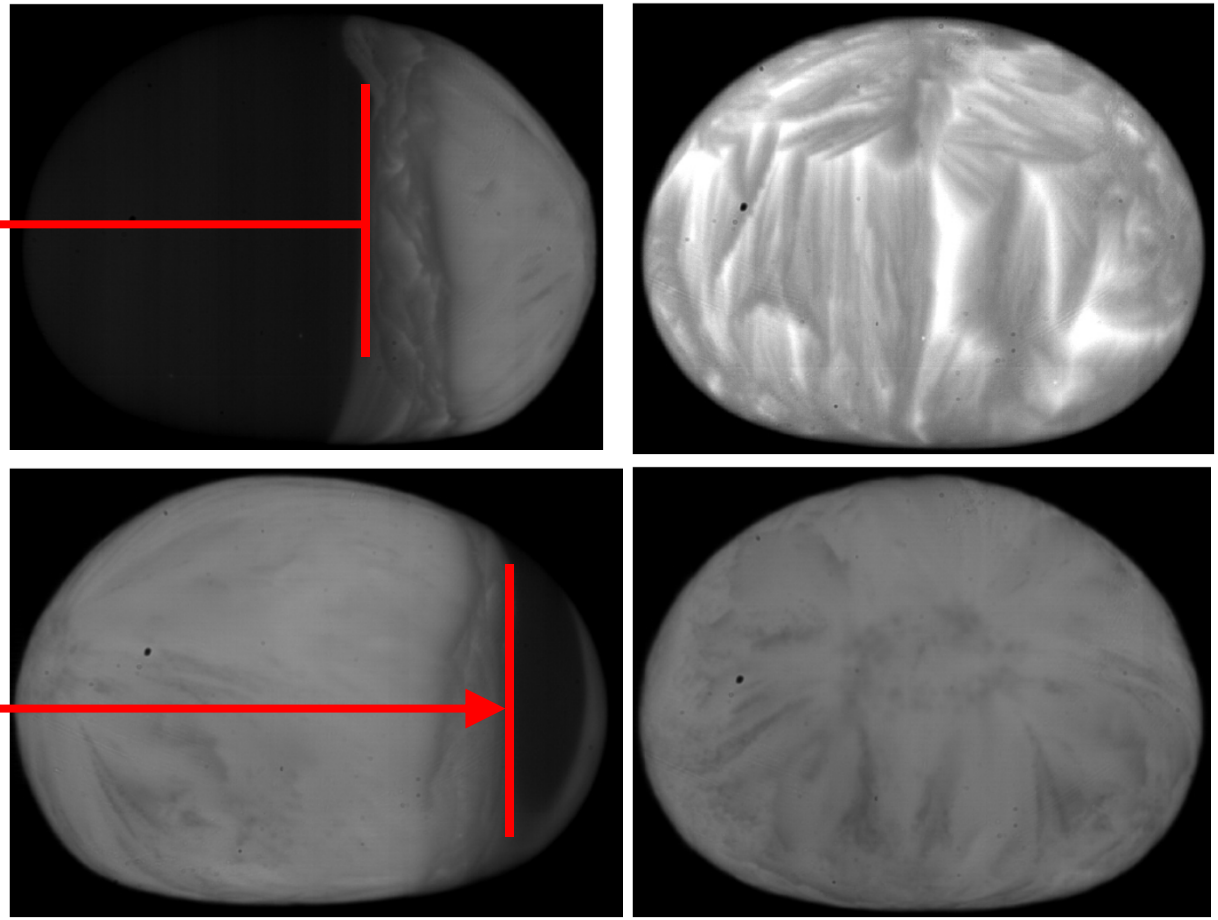

270 picture
t = 0.103 sec
Δx ≈ 0.15 cm
v ≈ 1.5 cm/s

Crystallization Rate of Liquid $Y_3Al_5O_{12}$ at ~1200°C

$Y_3Al_5O_{12}$ YAG

Known Melting Point of YAG 1942°C → Calculation of ε

$$\frac{1}{T}-\frac{1}{T_a}=\frac{\lambda}{C_2}\ln(\varepsilon_\lambda)$$

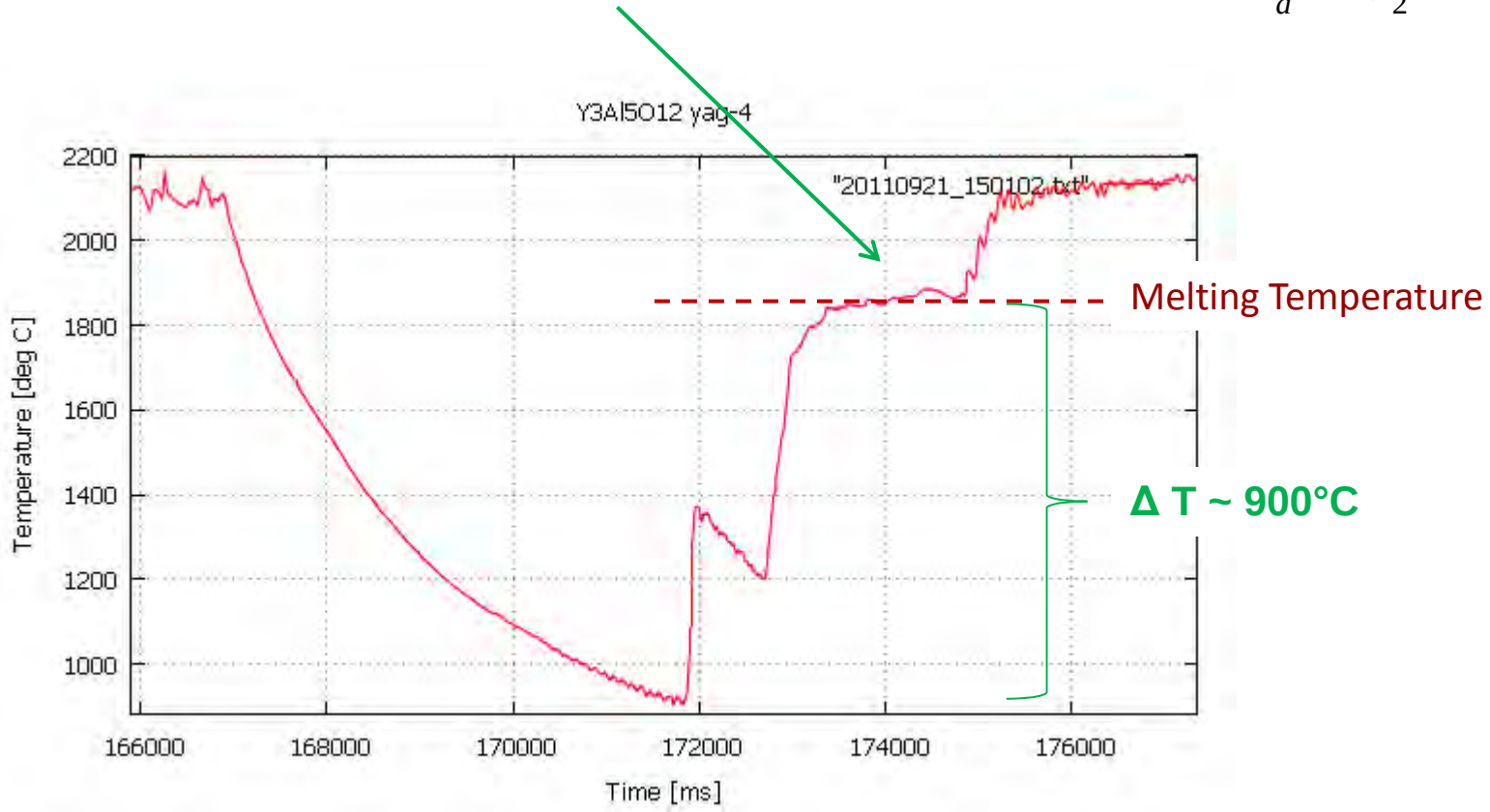

$Y_3Al_5O_{12}$ YAG

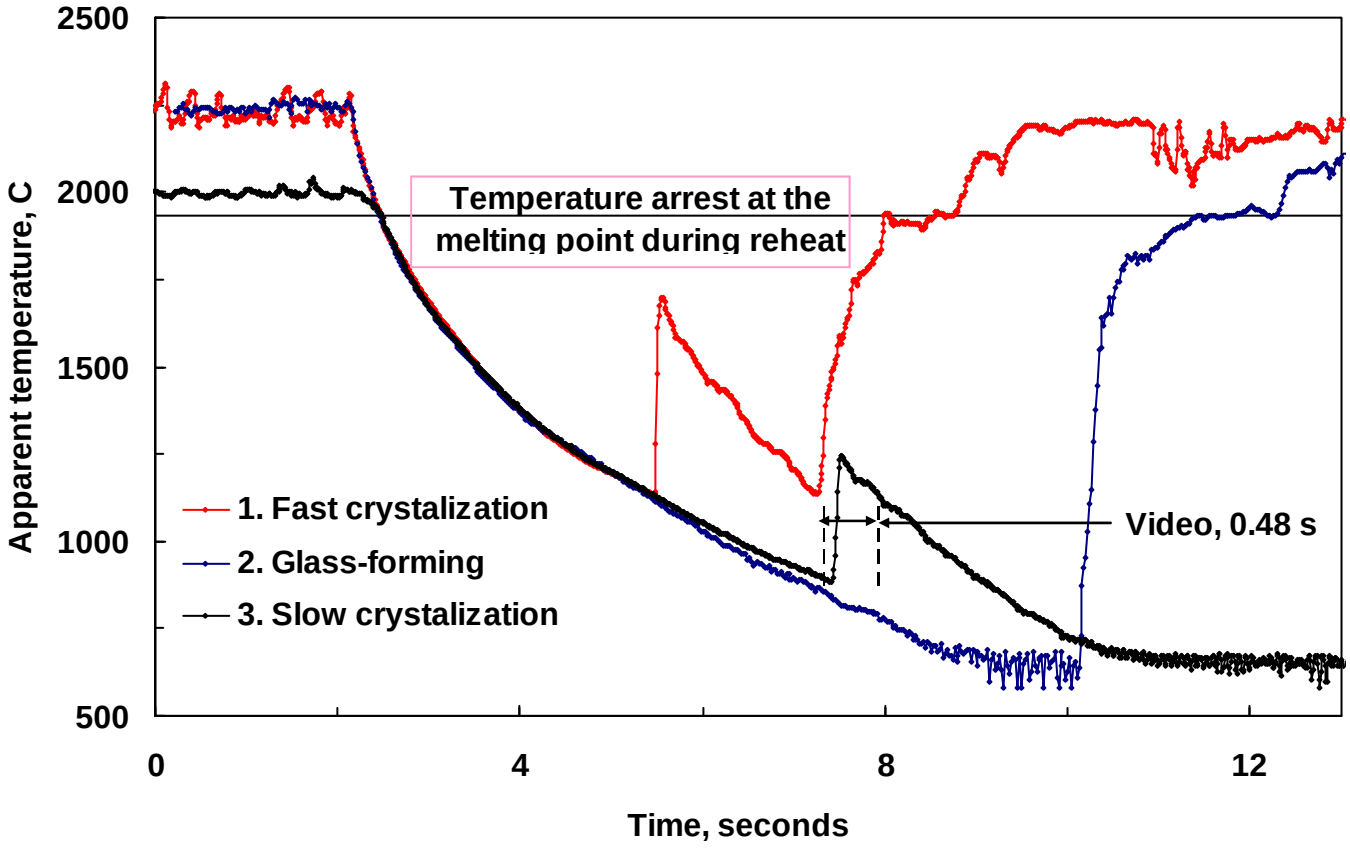

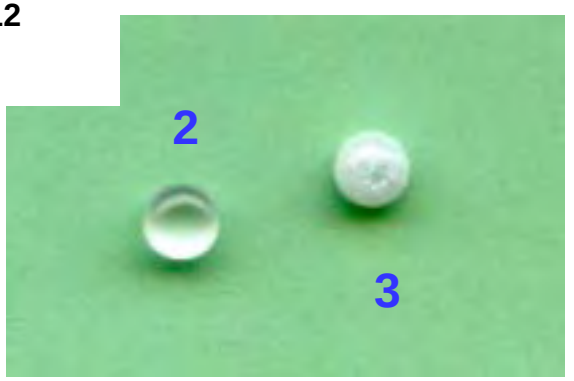

$Y_3Al_5O_{12}$: Different Cooling Conditions

$Y_3Al_5O_{12}$ YAG : Microstructure

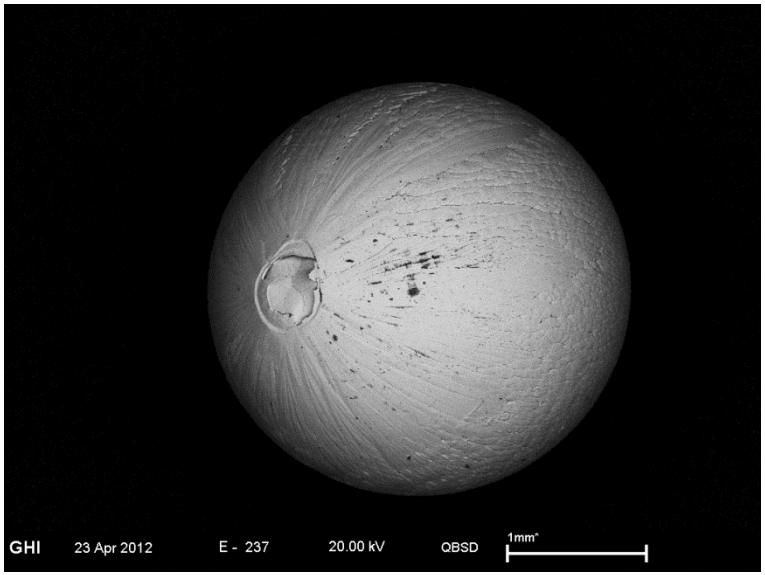

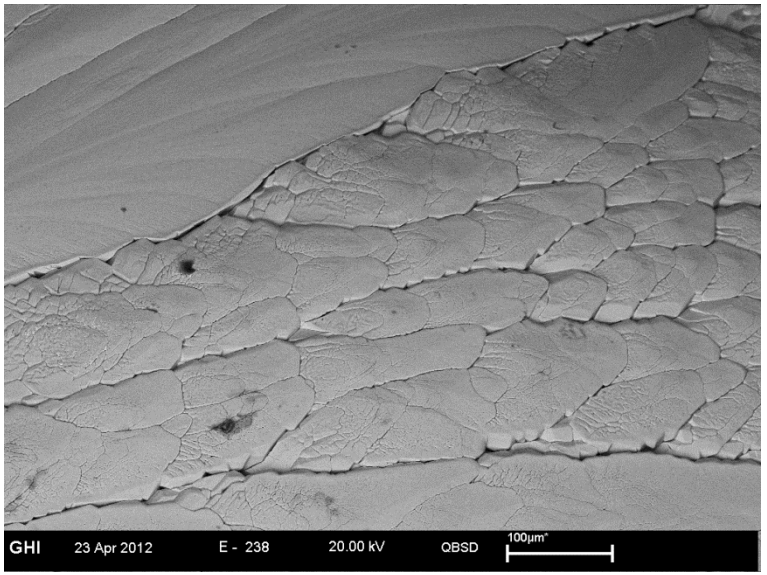

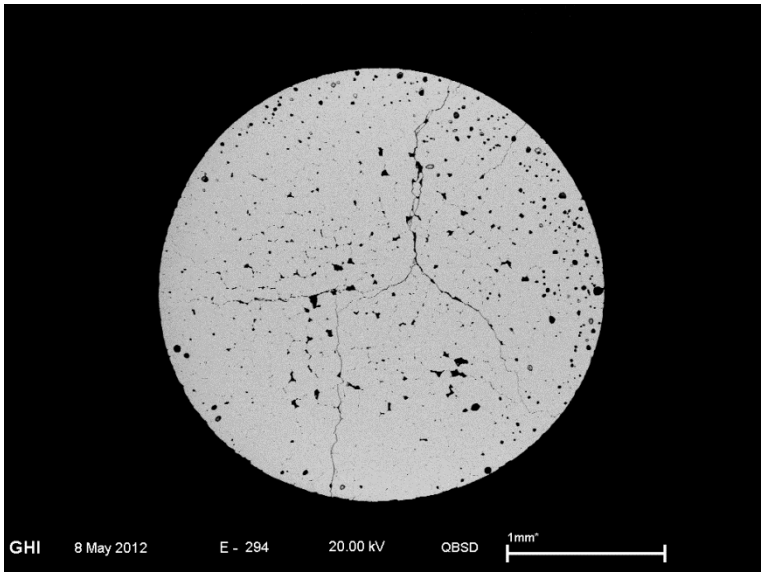

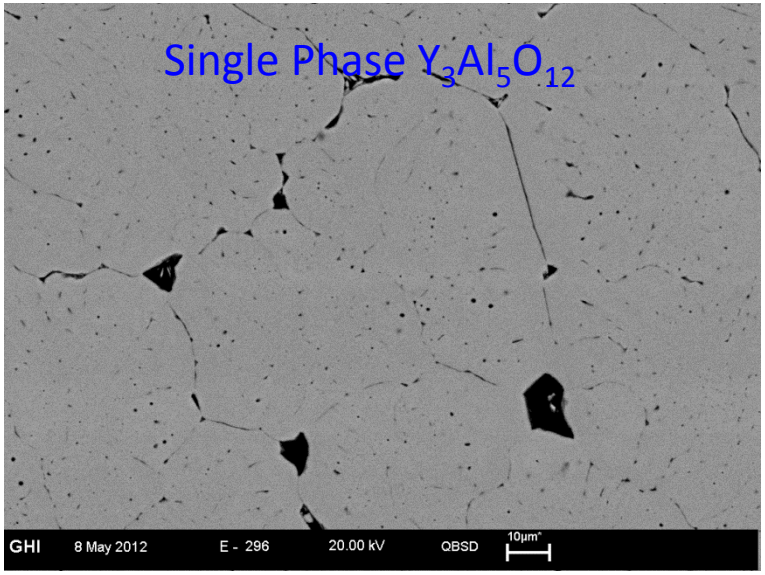

$Y_3Al_5O_{12}$ YAG

Out of Equilibrium ?

$Y_3Al_5O_{12}$ YAG

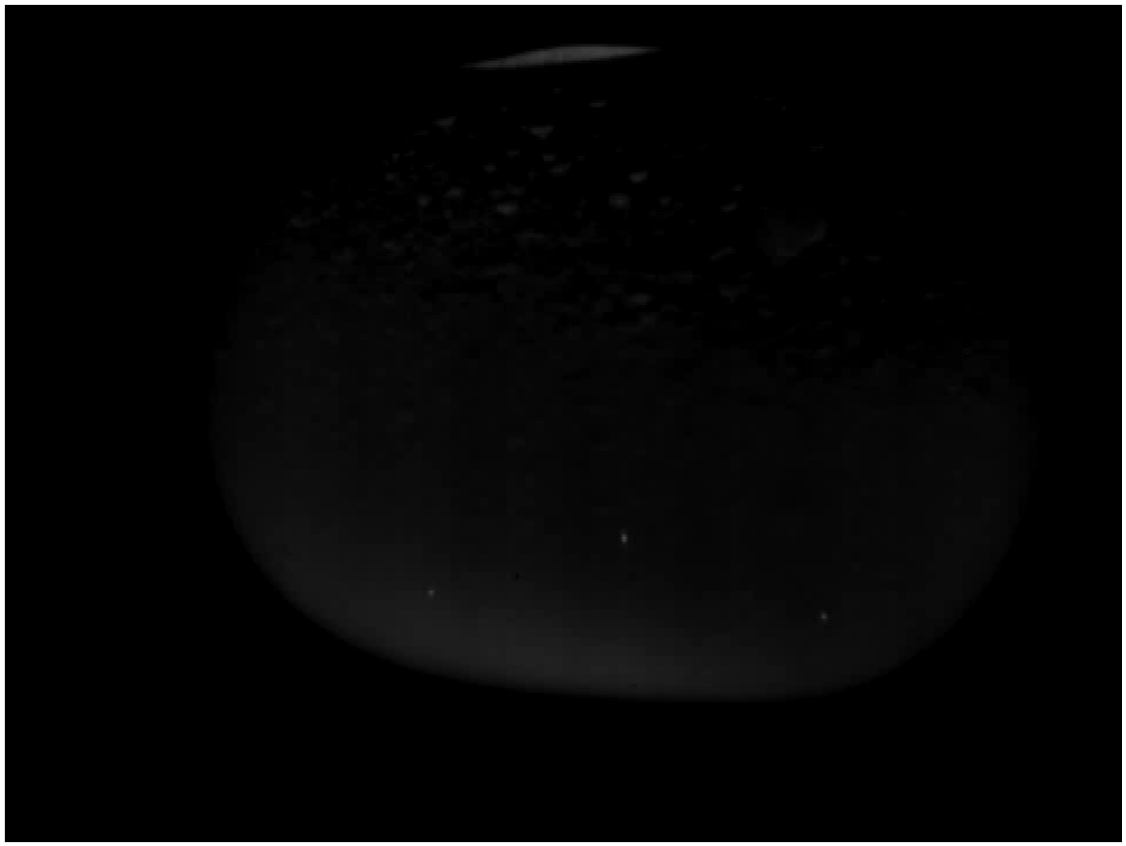

Out of Equilibrium ?

$Y_3Al_5O_{12} – Al_2O_3$ Eutectic

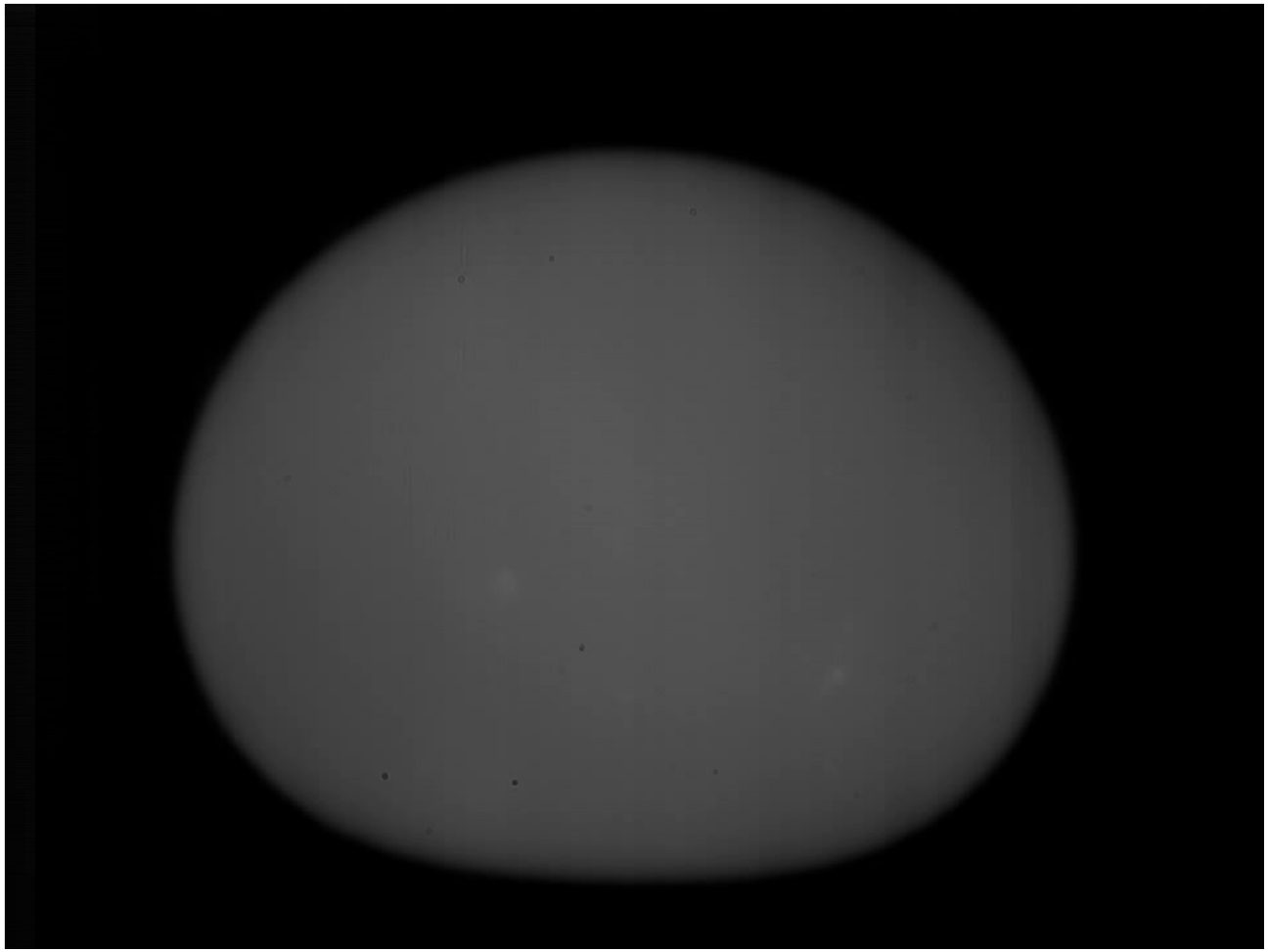

Undercooling, Recalescence and Crystallization of $Y_3Al_5O_{12} – Al_2O_3$ Eutectic Composition

$Y_3Al_5O_{12} – Al_2O_3$ Eutectic

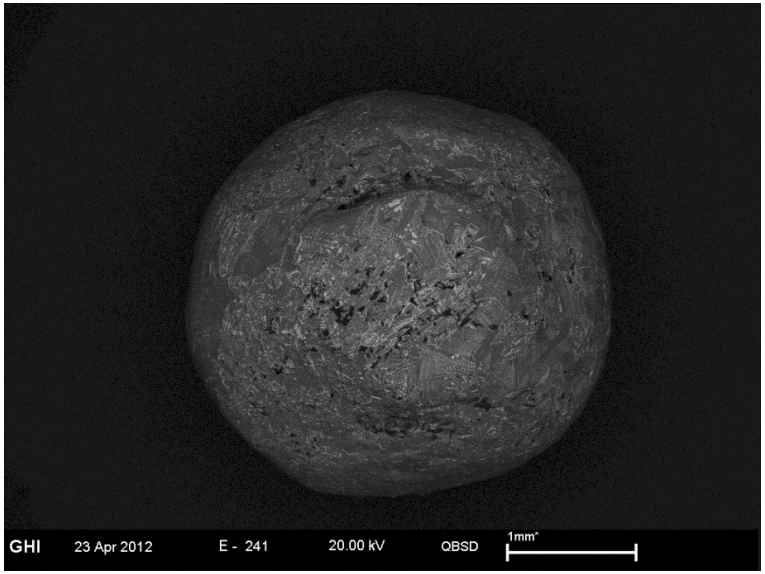

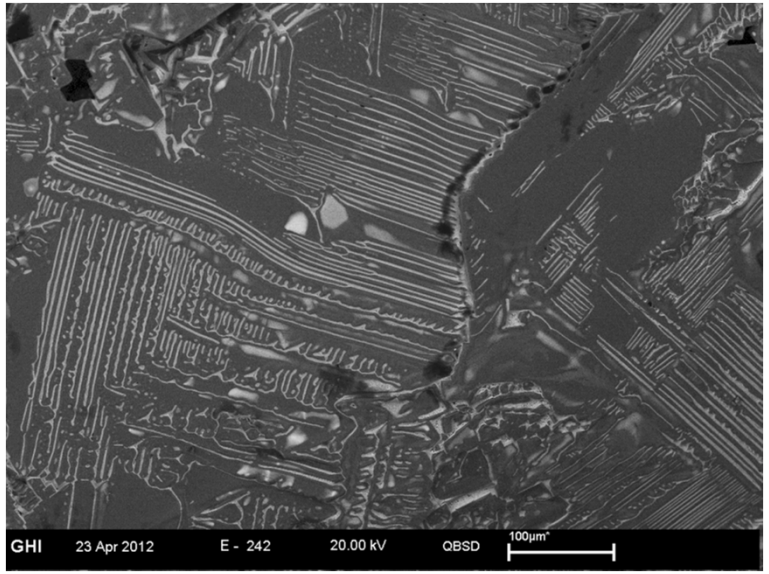

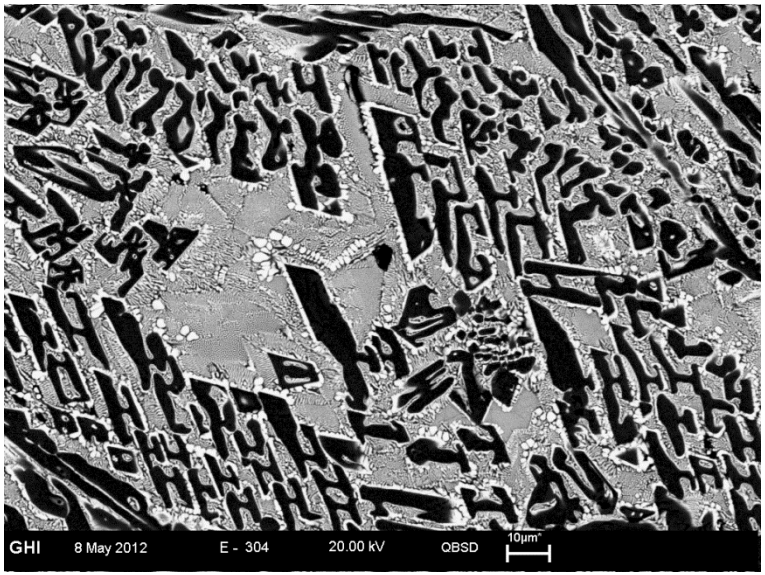

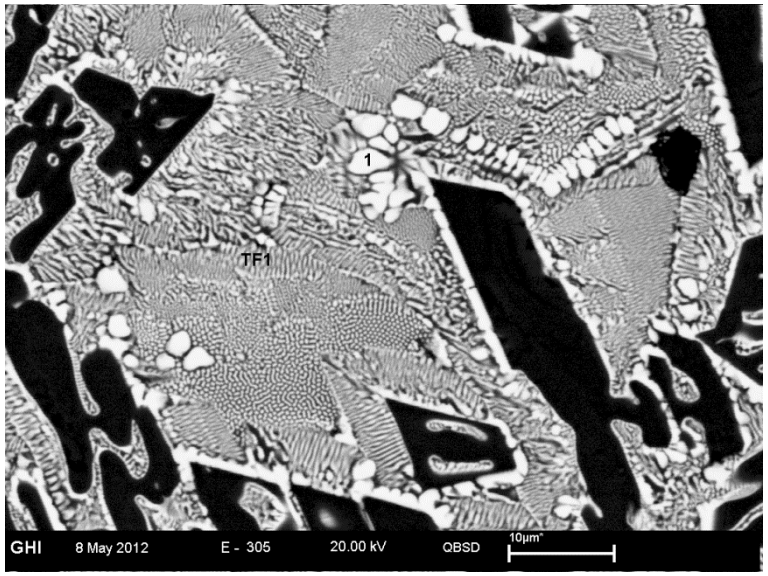

High Temperature Phase Transitions

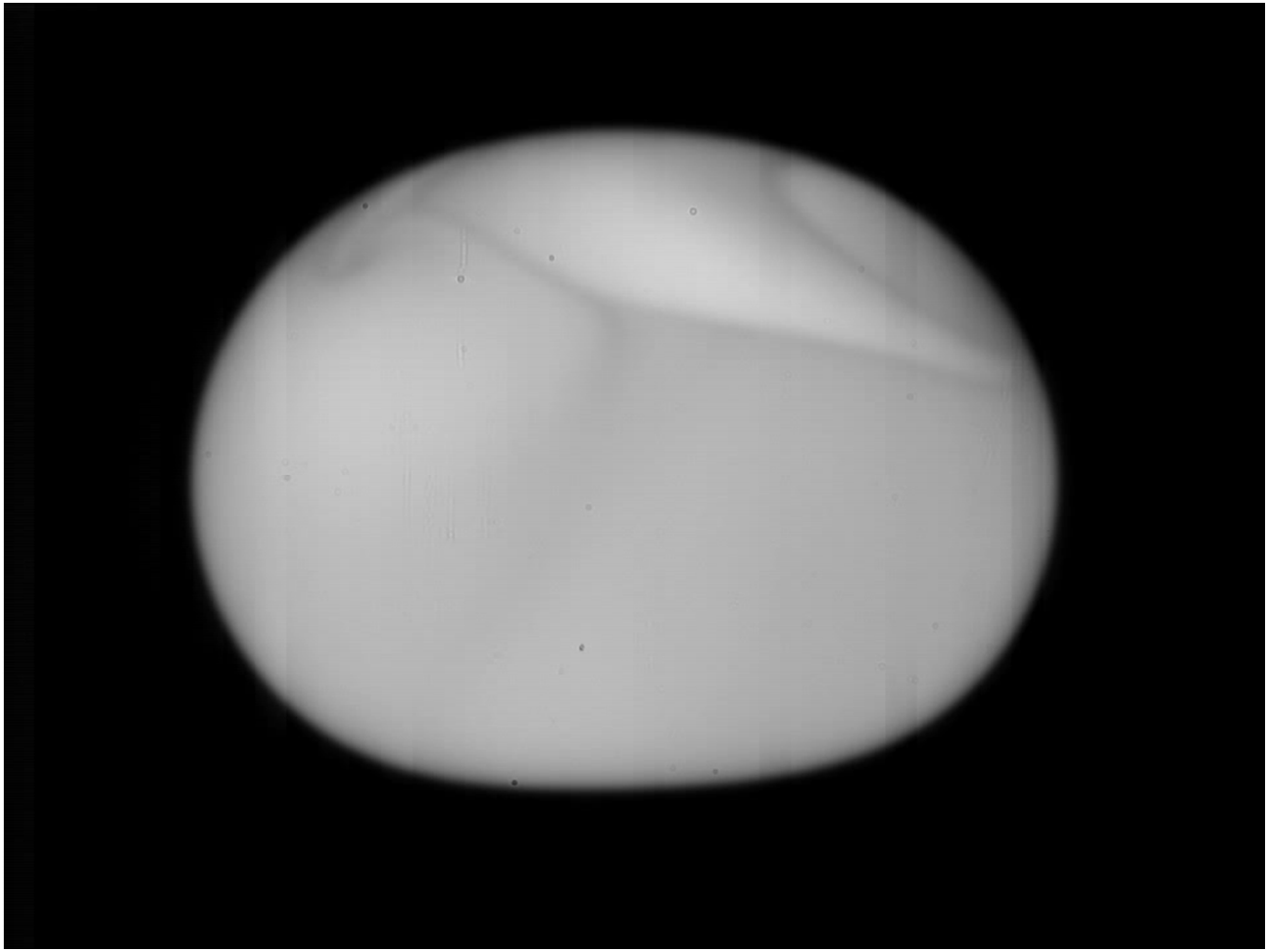

Undercooling, Recalescence and Crystallization of Y_2O_3

High Temperature Phase Transitions

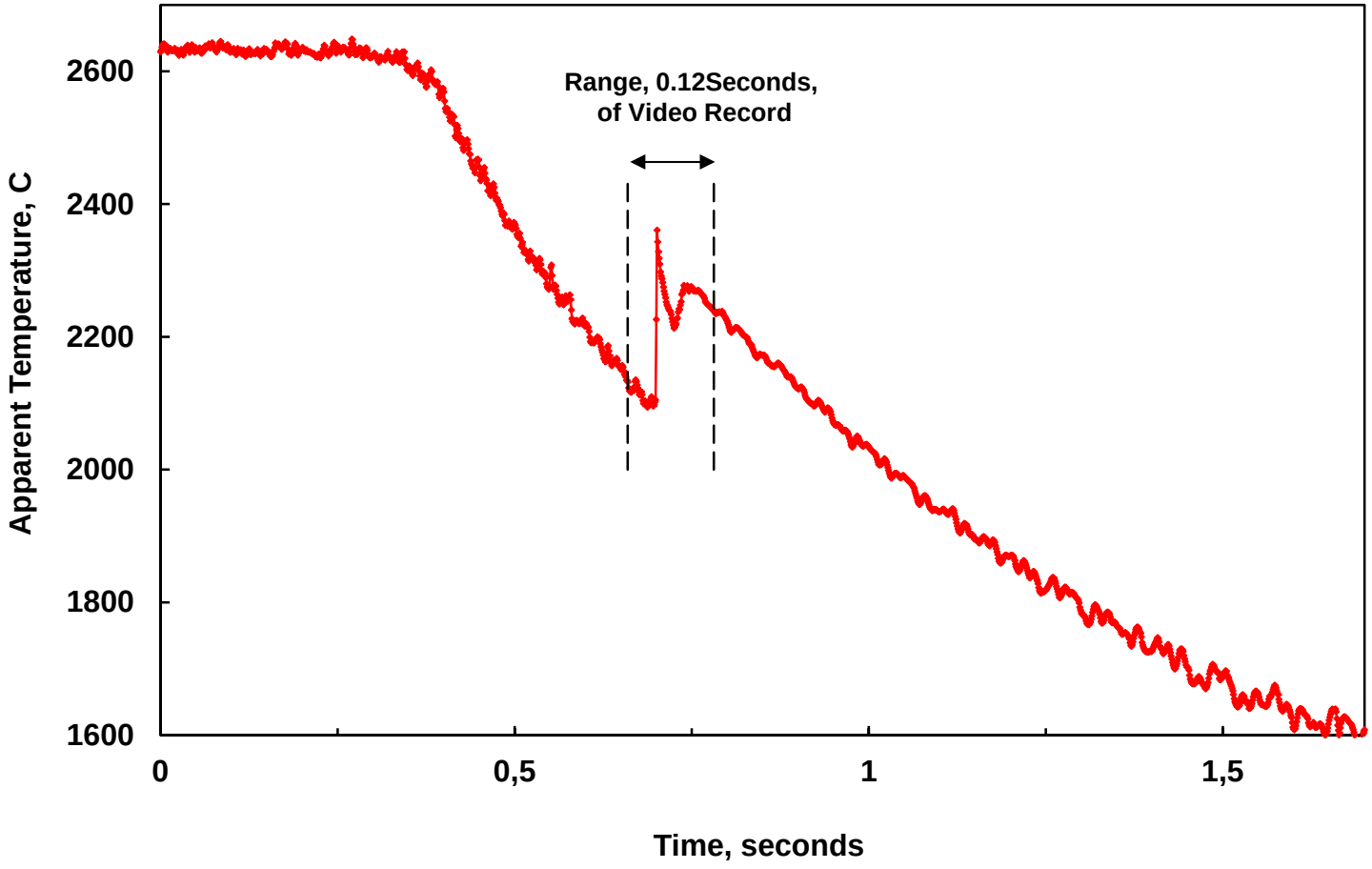

Y_2O_3 Cooling Curve

High Temperature Phase Transitions

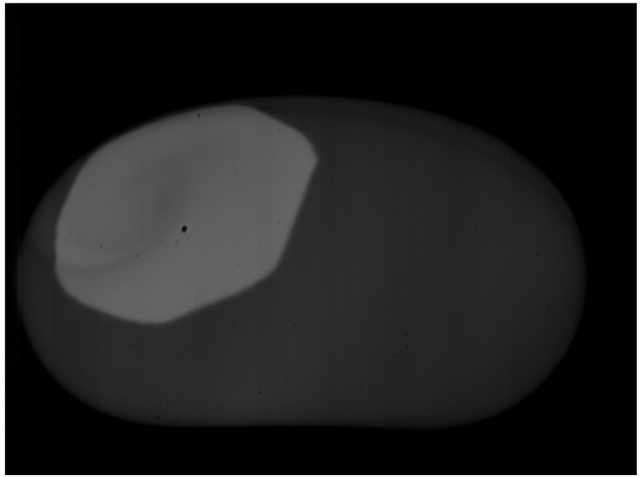

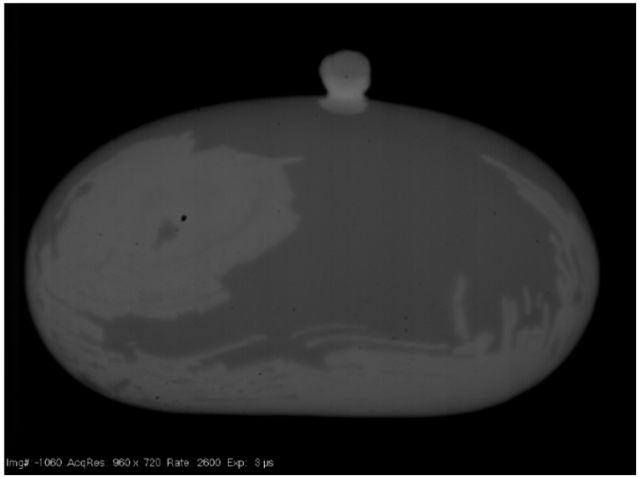

1 Rotation, 35 ms

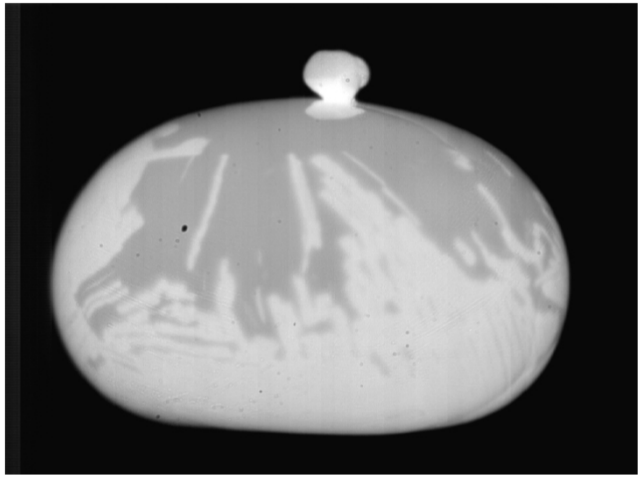

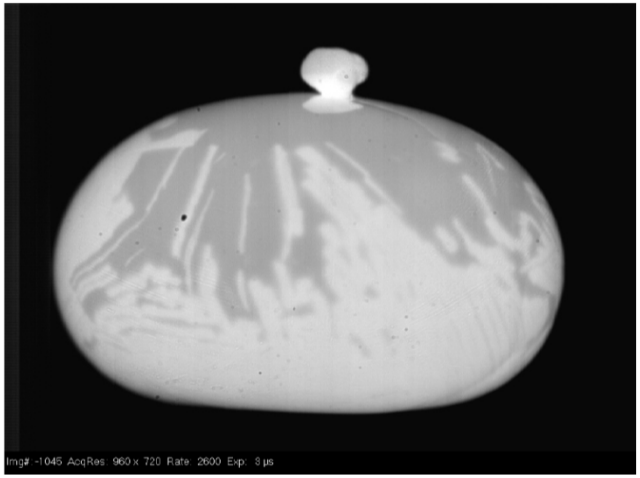

385 µs

Oxygen-Yttrium Phase Diagram

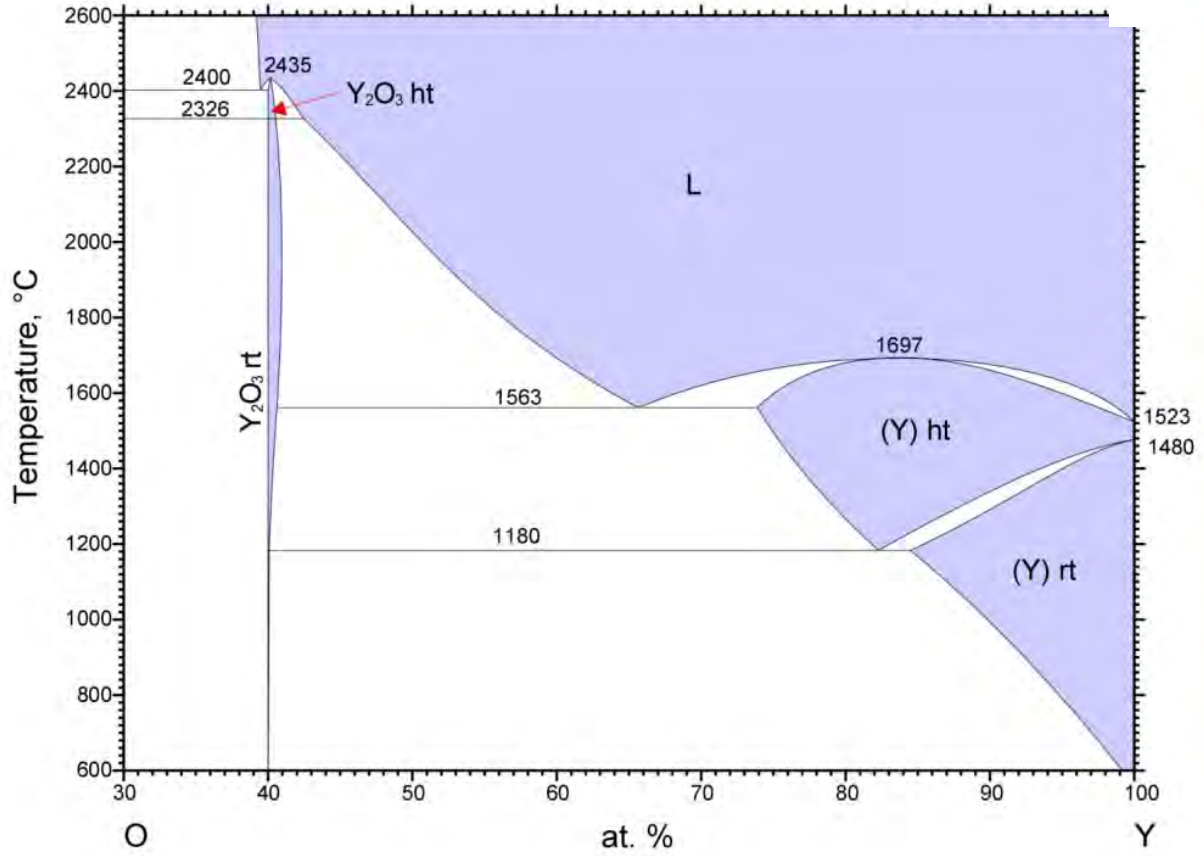

A. Boudene et al. : "Thermochemical Measurements and Assessment of the Phase Diagrams in the System Y-Ba-Cu-O", High Temp. Mater. Sci. **35** (1996) 159–179.

Phase	Space Group	Stability Range	Density	Volume
		°C	g/cm³	nm³
Cubic (rt)	$Ia\bar{3}$	RT-2326	5.03	1.119230
Hexagonal (ht)	$P6_3/mmc$	2326-2435	4.90	0.0766

High Temperature Phase Transition

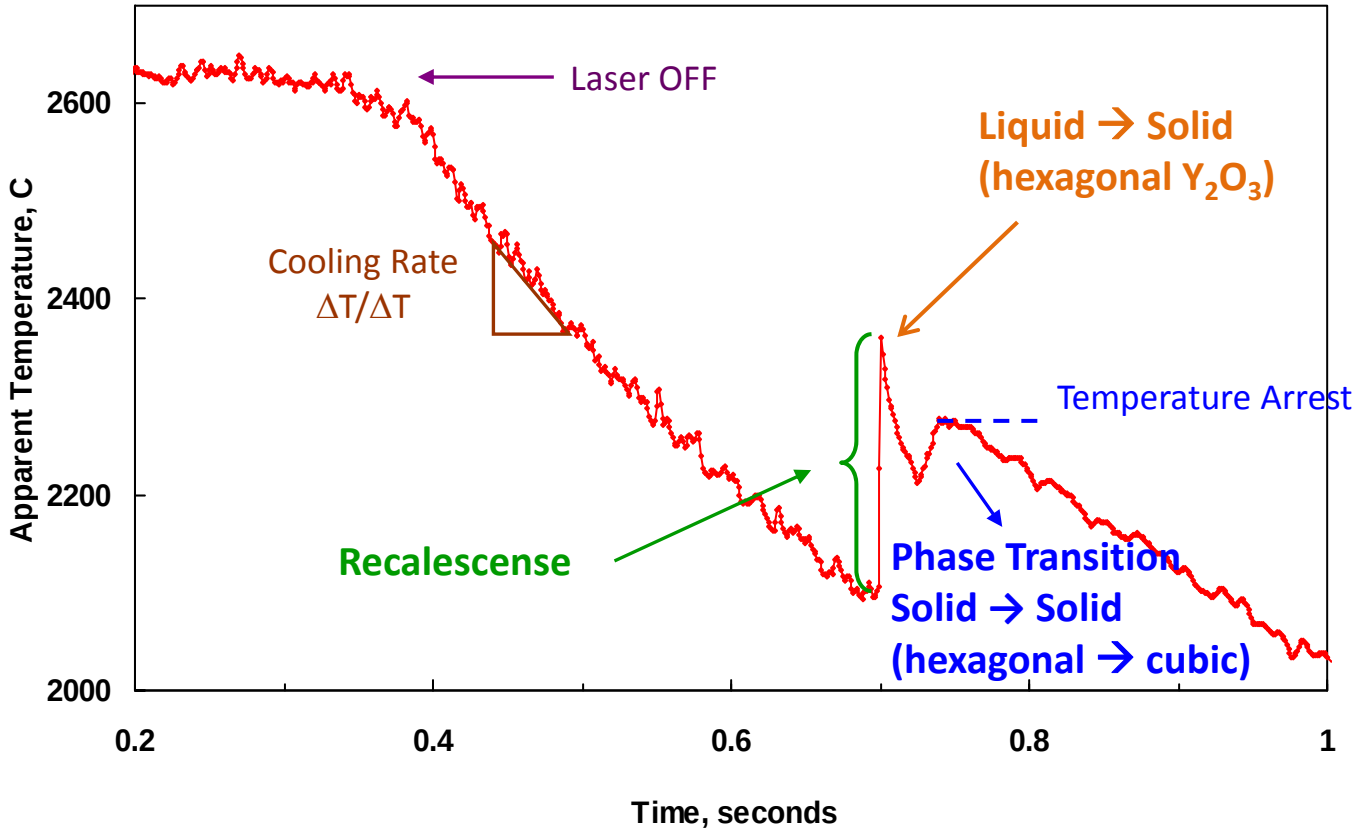

Y_2O_3 Cooling Curve

→ Crystallization of Y_2O_3 followed by Phase Transition

High Temperature Phase Transitions

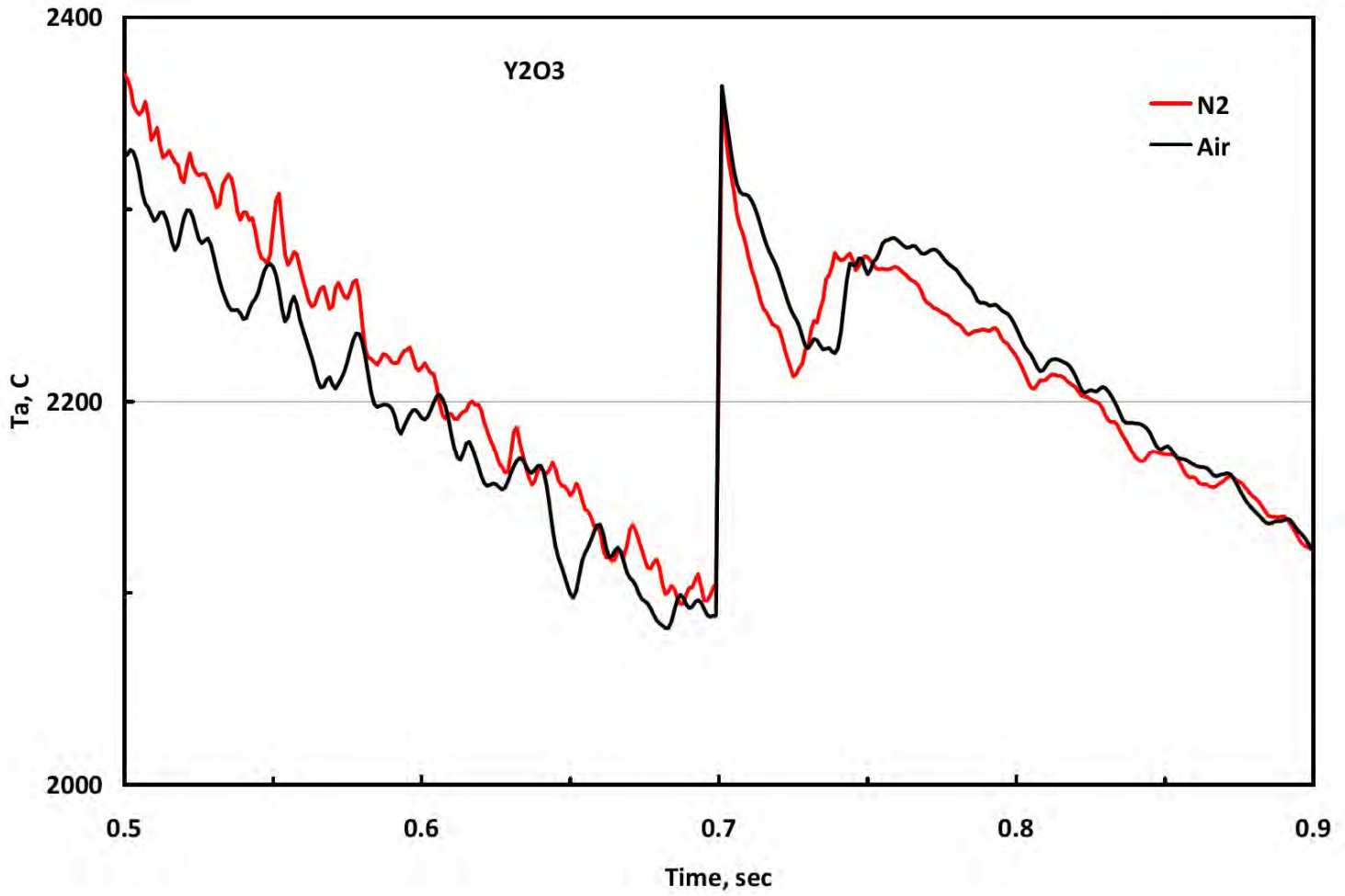

Surface Tension and Viscosity

Vibration of a Spherical Droplet:

Frequency [1] :

$$f_l^2 = \frac{l(l-1)(l+2)\gamma}{3\pi m}$$

Damping [2] :

$$\tau_l = \frac{\rho R_0^2}{(l-1)(2l+1)\mu}$$

f = Resonance Frequency
T = Time-Constant
l= 2,3,.. Order Number of the Vibration (Resonance-Modes)
γ = Surface Tension
μ = Viscosity
ρ = Density
R_0 = Radius of Melt Droplet
m = Mass of Melt Droplet

[1] J. W. S. Rayleigh, Proc. Royal Soc. of London, 29, 71-79 (1879)
[2] H. Lamb, Proc. London Math. Society, 13, 51-66 (1881)

- Modulation of the Acoustic Forces on Levitated Liquid Drops over the Range of Frequencies where Resonant Oscillation can be observed → Measuring Resonant Frequencies → γ
- Induction and Measuring Dynamic Oscillation in Overheated and Undercooled Liquids at very High Temperature → Observing the Decay of Oscillations → μ

Advantage of Aero-Acoustic Levitation → Interference from acoustic forces are small since they can be made very small compared with the surface tension forces on liquid drops

Manipulation of a Water Droplet

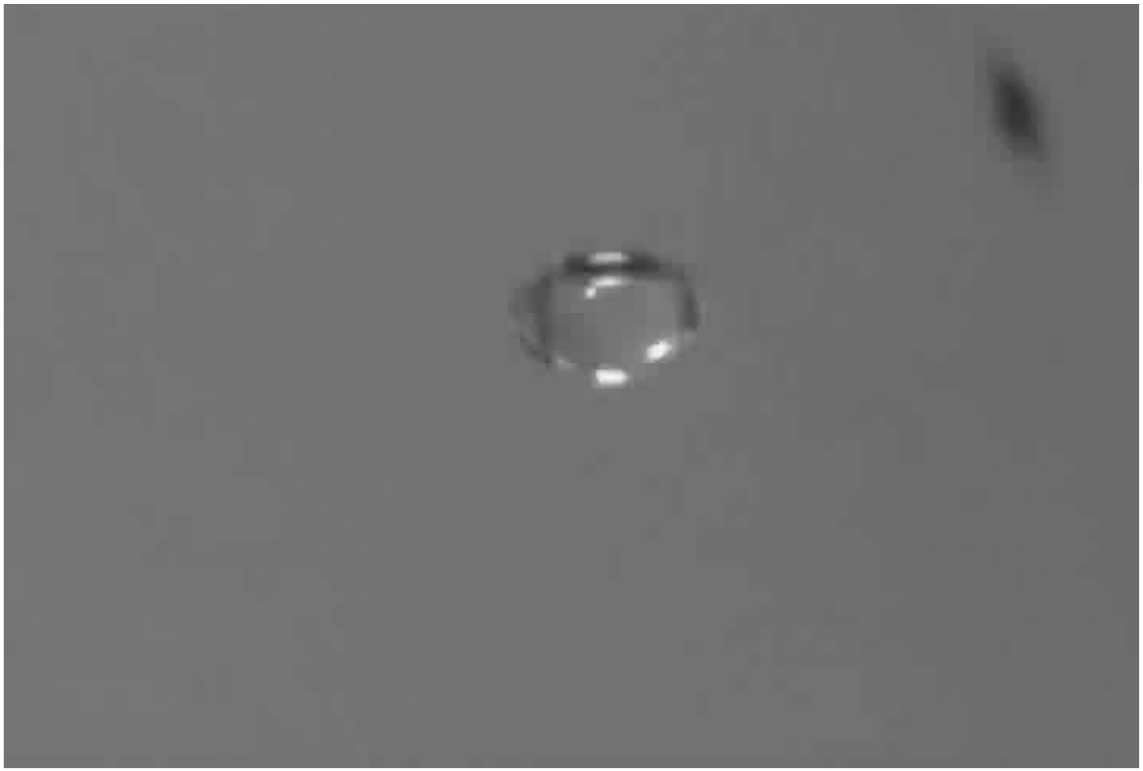

Surface Tension and Viscosity

Position-Sensors on the Control Screen:

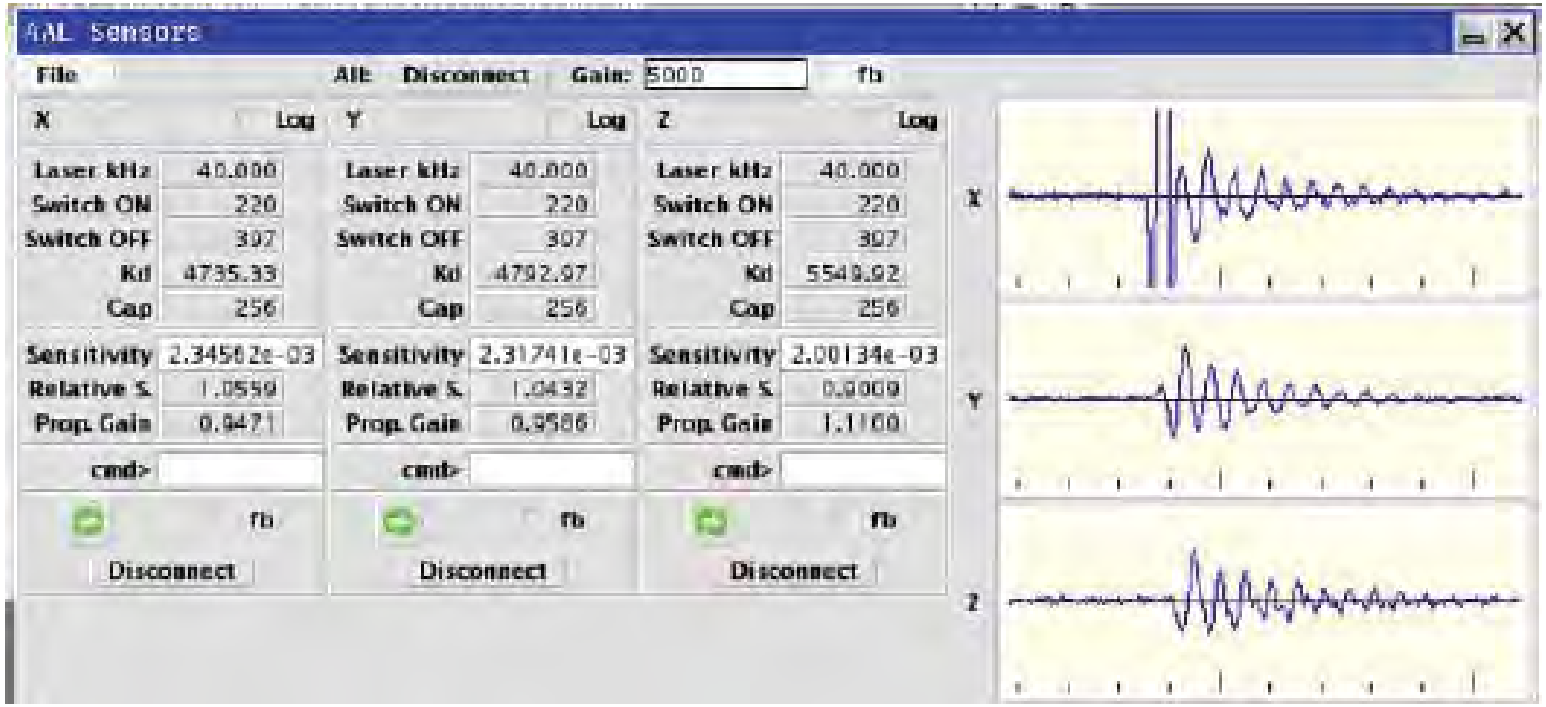

Relaxation of a Levitated Water Droplet
F ≈ 20 Hz

Surface Tension and Viscosity

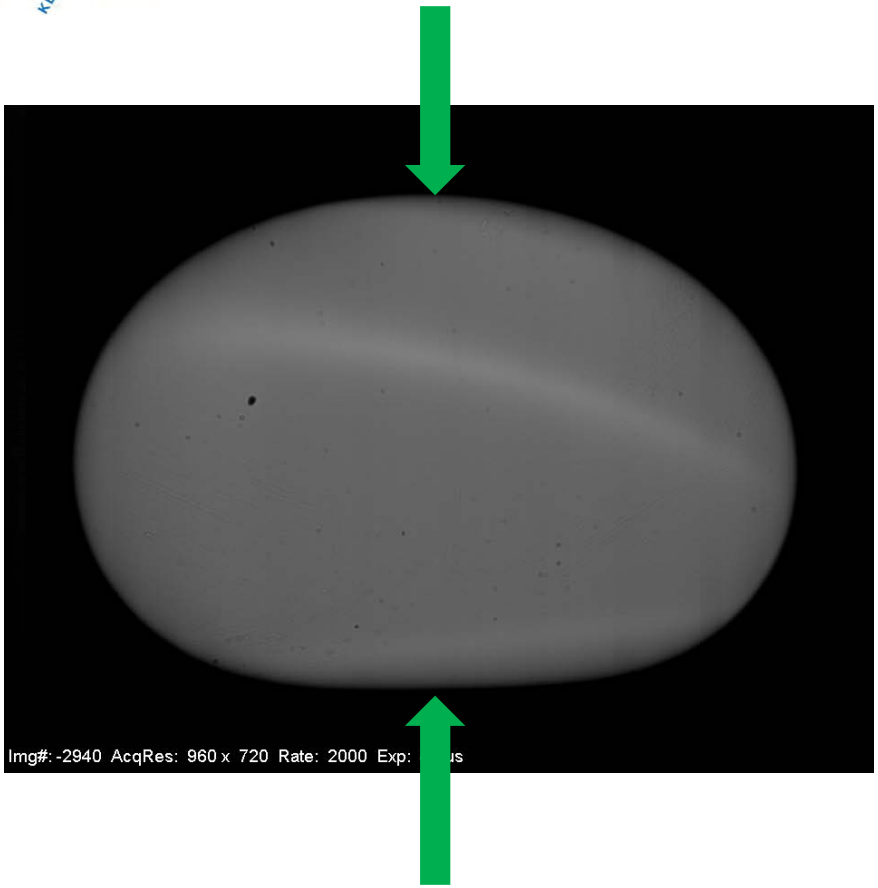

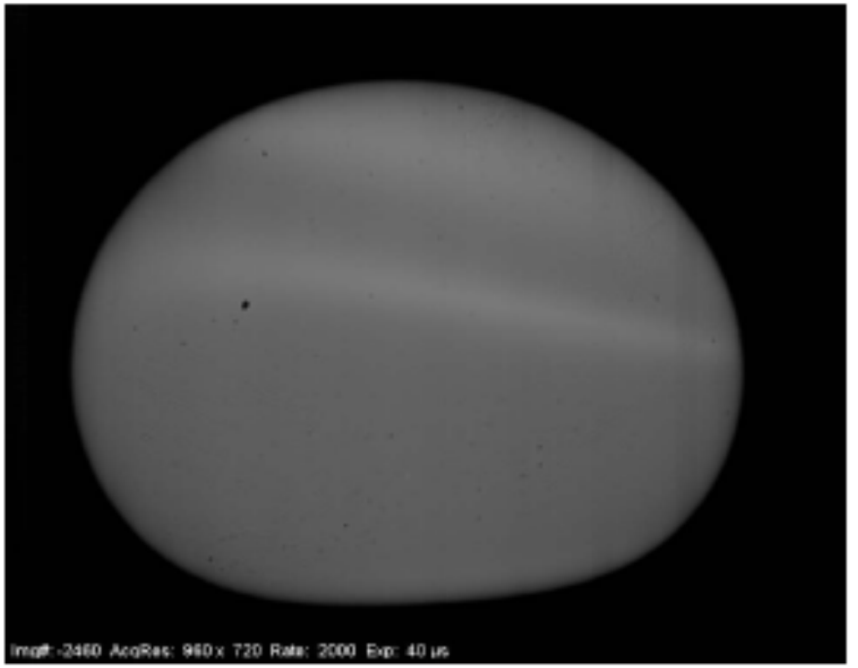

Compression by Acoustic Forces

Relaxation

Undercooled YAG-Melt ($Y_3Al_5O_{12}$), T_a = 1700°C

Surface Tension and Viscosity

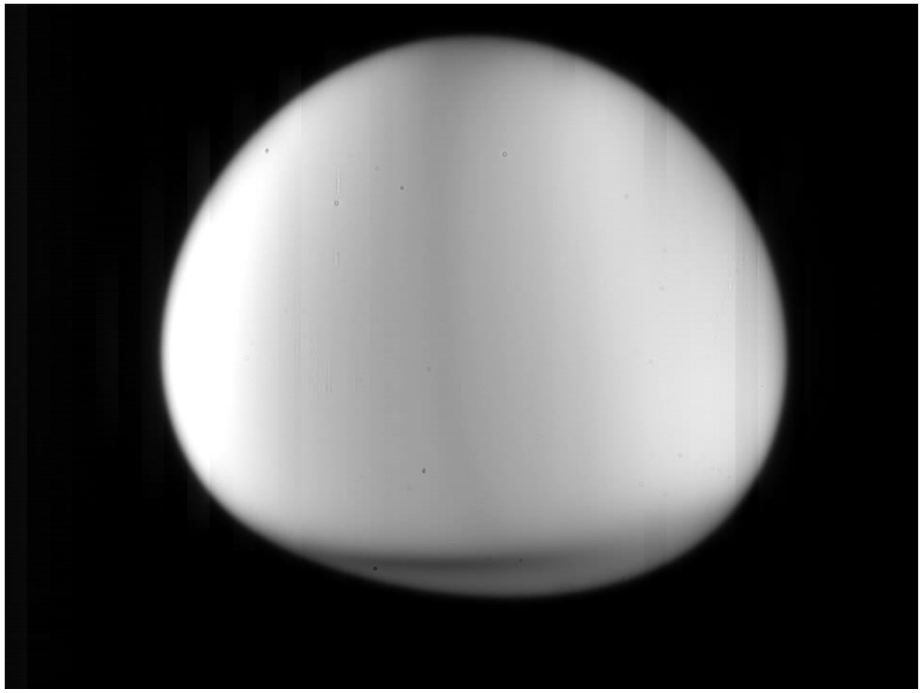

Dynamic Oscillation of Liquid Al_2O_3 at ~1900°C

Surface Tension and Viscosity

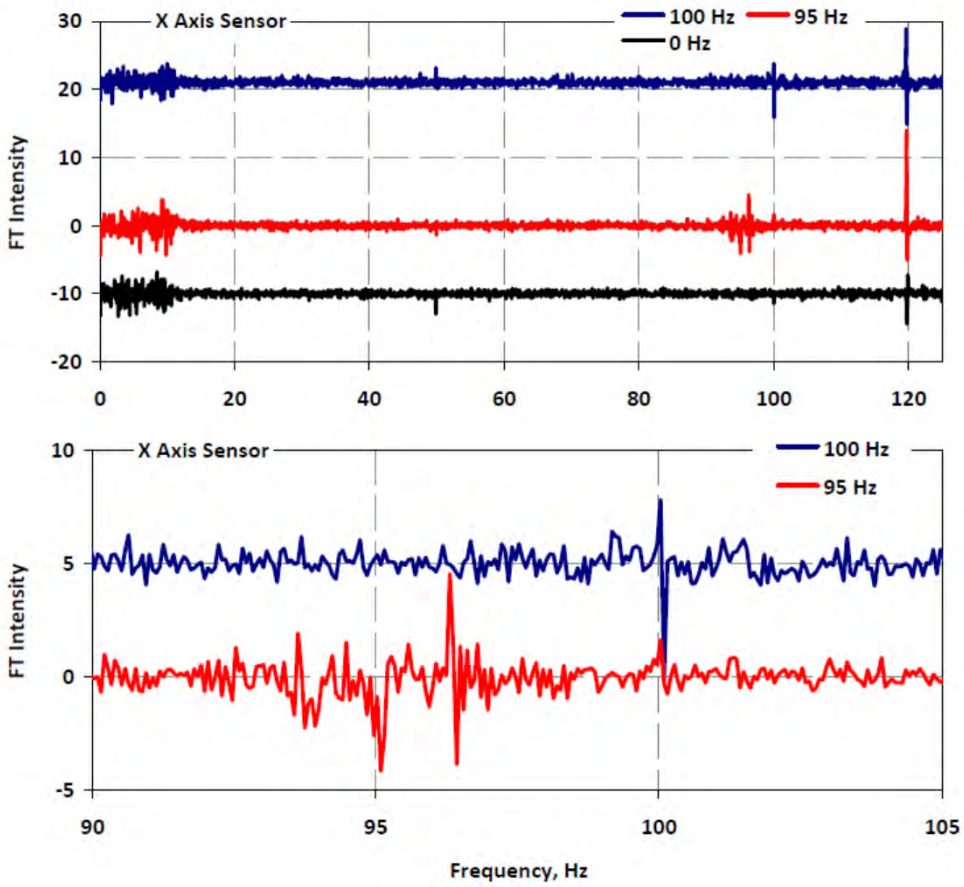

Fourier analysis of X-axis sensor data with a levitated 67 mg liquid aluminum oxide sample and with the output of the X-A transducer

- 95Hz Experiment → Peak at 96.4 Hz close to resonant shape oscillation of the liquid sample (+ 95 Hz oscillation of the acoustic intensity)
- 96.4 peak is not seen when the modulation is at 100 Hz → Modulation with 100 Hz was not close enough to excite 96.4 Hz Peak → Continuous scan over a range of frequencies

Aero-Acoustic Levitator Demonstration

Thank You Very Much For Your Attention !!!